d·Collection

A THESIS FOR THE DEGREE OF MASTER OF SCIENCE

Molecular aspects and functional characterization of Cystatin B and Glutaredoxin-1 from two commercially important teleostean species interpreting the impact on host immunity

Pasquelge Don Sachith Udara Wickramasinghe

Department of Marine Life Sciences

GRADUATE SCHOOL

JEJU NATIONAL UNIVERSITY

REPUBLIC OF KOREA

February 2017

MOLECULAR ASPECTS AND FUNCTIONAL CHARACTERIZATION OF CYSTATIN B AND GLUTAREDOXIN-1 FROM TWO COMMERCIALLY IMPORTANT TELEOSTEAN SPECIES INTERPRETING THE IMPACT ON HOST IMMUNITY

Pasquelge Don Sachith Udara Wickramasinghe

(Supervised by Professor Jehee Lee)

A thesis submitted in partial fulfillment of the requirement for the degree of

MASTER OF SCIENCE

February 2017

This thesis has been examined and approved by

....
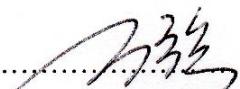
Thesis Director, **Qiang Wan** (PhD), Research Professor,

Fish Vaccine Research Center, Jeju National University.

....
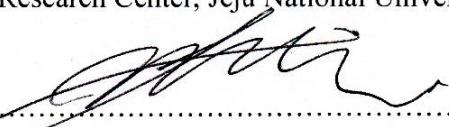
Chulhong Oh (PhD), Associate Professor of Marine Biology,

Department of Marine Biology, University of Science & Technology

....

Jehee Lee (PhD), Professor of Marine Life Sciences,

School of Marine Biomedical Sciences, Jeju National University

Date: 01.12.2016

Department of Marine Life Sciences

GRADUATE SCHOOL

JEJU NATIONAL UNIVERSITY

REPUBLIC OF KOREA

Acknowledgments

The current thesis would not be a reality with the immeasurable support and assistance from many individuals and this note is an extension of my appreciation and gratitude towards them.

First, I would like to thank the Almighty God for His ultimate blessings and guidance in giving me the strength, protection, and wisdom to successfully finish the study.

I thank my supervisor Professor Jehee Lee of the Department of Marine Bio Medical Sciences at Jeju National University, South Korea. He was always available whenever I ran into a trouble spot or had a question about my research or writing. He consistently allowed the thesis to be my own work but steered me in the right the direction whenever he thought I needed it.

I would also like to thank the experts who were involved in the thesis defense as committee members for this research project: Dr. Qiang Wan, Research Professor, Jeju National University and Dr. Chulhong Oh, Associate Professor of Marine Biology, University of Science & Technology. Without their passionate participation and input, it could not have been validated. Also, I profusely convey my sincere thanks to all the professors of my department for their encouraging guidance in the field of Marine Life Sciences.

My sincere gratitude reaches out for the past and present members of the Marine Molecular Genetics Laboratory (MMGL), Dr. N. Umasuthan, Dr. D.A.S. Elvitigala, Dr. S.N.D.K Bathige, Dr. William Shanthakumar Thulasitha, Dr. Mingyoung Kim, Dr. Shin, Dr. Sukkyoung Lee, Dr. Yucheol Kim, Mr. Thiunuwan Priyathilaka, Mr. G.I. Godahewa, Mr. Neranjan Tharuka, Mr. H.M.L.B.P. Herath, Mr. J.D.H.E. Jayasinghe, Mr. V. Udayantha, Ms. N.C.N. Perera, Mr. R. Kugapreethan, Mr. J. Nilojan, Mr. A. Pavithiran, Mr. Seongdo Lee, Ms. Minyoung Oh, Ms. Sunhye Kang, Ms. Jeongin Ma, Ms. Jiyeon Ko, Ms. Eunyoung Jo, Mr. Hyukjae Kwon, Ms. Hyerim

Yang, Ms. Jeongeun Kim, Mr. Hanchang Sohn, and Ms. Gabin Kim, for their support and care in laboratory work. Also, I wish to express my appreciation to all the Sri Lankan and International friends of Jeju National University International Students' Organization (JISO) for making my university life interesting during the two year period.

I'm sincerely grateful for Prof. Young-hoon Kang the Dean of the Center for International Affairs, Jeju National University and all the staff members for the support and the hospitality shown towards me during my study period.

Brain Korea (BK) 21-plus scholarship programme; Development of Fish vaccines and human resource training-funded by Ministry of Oceans and Fisheries, Korea; National Institute of Fisheries Science, Korea; the Golden Seed Project (GSP), The Ministry of Oceans and Fisheries are also included in my gratitude for providing funds to conduct my research without any hassle.

Also, I wish to express my acknowledgment to Prof. R. S. Dassanayake and Dr. N. V. Chandrasekharan of Department of Chemistry, University of Colombo, Sri Lanka for their recommendation and the support to get the opportunity and to pursue my masters at Jeju National University.

Finally, I must express my very profound gratitude to my parents for providing me with unfailing support, blessings and continuous encouragement throughout my years of study and through the process of researching and writing this thesis. This accomplishment would not have been possible without them. Thank you.

………………………..
P. D. S. U. Wickramasinghe

Dedicated to my Ever-loving beloved parents

TABLE OF CONTENTS

SUMMARY

Aquaculture has become one of the leading world industries with its rapid growth arising from the demand from the vast consumption market. However, fueled by rising domestic income, consumers in emerging economies are experiencing a diversification of the types of available fish through an increase in fishery imports. This significant growth in fish consumption has enhanced people's diets around the world through diversified and nutritious food. Fish is usually high in unsaturated fats and provides health benefits in protection against cardiovascular diseases. It also aids fetal and infant development of the brain and nervous system. With its valuable nutritional properties, it can also play a major role in correcting unbalanced diets and, through substitution, in countering obesity. In 2013, fish accounted for about 17 percent of the global population's intake of animal protein and 6.7 percent of all protein consumed. With the aforementioned concept on mind, the current research was conducted to provide an insight into the immune system of two commercially important fish species.

Cystatins are a large superfamily of proteins involved in the competitive reversible inhibition of C1 class cysteine proteases. Plant derived papain proteases and cysteine cathepsins are the major cysteine proteases that interact with cystatins. Cystatins superfamily can be further clustered into three groups as Stefins, Cystatins and Kininogens. Among them cystatin B is placed under Stefins. The cystatin B lacks a signal sequence, disulfide bonds or carbohydrate groups. However, it contains the conserved cystatin family signature including single cystatin like domain, cysteine protease inhibitory signature concealing pantapeptide (QXVXG) consensus sequence and N-terminal two conserved neighboring glycine (8GG9) residues. In the current study, a member of cystatin B was identified from Korean black rockfish (*Sebastes schlegeli*) using a cDNA database and designated as RfCytB. The full length cDNA of RfCytB consisted of 573 bp, with a

coding region of 294 bp. The 5´-untranslated region (UTR) comprised of 55 bp, and 3´-UTR of 263 bp consisting a polyadenylation signal sequence and a polyA tail. The coding sequence encodes a polypeptide consisting of 97 amino acids with a predicted molecular weight of 11 kDa and theoretical isoelectric point of 6.3. The RfCytB shared homology features with other teleost and vertebrate species and was clustered with the Cystatin family 1 in our phylogenetic reconstruction. RfCytB was ubiquitously expressed in all tissue types of healthy animals with gill and spleen being the highest. Temporal expression of RfCytB displayed significant up-regulation upon infection with *Aeromonas salmonicida*. Recombinantly expressed RbCytB showed concentration dependent papain inhibitory activity with high thermal stability and transient expression of RfCytB in LPS activated murine macrophages induced the expression of genes related to pro-inflammatory conditions, such as iNOS and TNF α, providing evidence for its protease inhibitory and immunity relevant roles in host, respectively.

Reactive oxygen species (ROS) can be generated as by-products in all oxygenic organisms during aerobic metabolism. External or internal oxidants such as superoxide, hydrogen peroxide, and hydroxyl radicals, referred to as ROS, can result in oxidative damage to proteins, lipids, and nucleic acids. Cells possess many antioxidant enzymes, including catalase (CAT), superoxide dismutase (SOD), glutathione peroxidase (Gpx), thioredoxin peroxidase (Tpx), glutaredoxin (Grx), and thioredoxin (Trx) systems, to resist oxidative damage. Grxs and Trxs play important roles in maintaining intracellular thiolredox homeostasis by scavenging reactive oxygen species. However, only a few Grxs have been functionally characterized in teleostean species. In this study, we identified Glutaredoxin 1 (GLRX1) from Rock bream and investigated their connection to antioxidant defense.

In the current study, a member of Glutaredoxin 1 was identified from Korean black rockfish (*Sebastes schlegeli*) using a cDNA database and designated as RbGLRX1. The full length cDNA of RbGLRX1 consisted of 833 bp, with a coding region of 318 bp. The 5´- untranslated region (UTR) comprised of 24 bp, and 3´-UTR of 491 bp. The coding sequence encodes a polypeptide consisting of 105 amino acids with a predicted molecular weight of 11.5 kDa and theoretical isoelectric point of 7.65. The RbGLRX1 shared homology features with other teleost and vertebrate species and was clustered mainly with other teleostean species in our phylogenetic reconstruction. RbGLRX1 was ubiquitously expressed in all tissue types of healthy animals with blood and liver being the highest. Temporal expression of RbGLRX1 displayed significant up-regulation upon infection with *Edwardsiella tarda*, *Streptococcus iniae* and by the rock bream iridovirus (RBIV). Recombinantly expressed RbGLRX1 exhibited concentration dependent alkyl and DPPH radical scavenging activities. Functional studies of RbGLRX1 gave positive results for insulin disulfide assay and classical HED assay thus proving its functional characteristics. Overall, the research provided valuable information on the role of RbGLRX1 on host immune defense against ROS.

LIST OF FIGURES

LIST OF TABLES

CHAPTER 1

1. INTRODUCTION

Edible marine fish are considered as protein rich source in human diets, thus farming of fish has been cherished recently to compensate the increasing demand on them. However, as a consequence of intensive culturing of large scale of fish in restricted areas, different stress factors, more prominently pathogenic stress have adversely affected to the yield of worldwide fish farming, resulting in considerable economic loss. Under the light of this background, investigations on molecular pathophysiology of mariculturable fish species can be considered as a primitive commencement of developing disease management strategies against the growing threat of pathogenic infections on them.

Black rockfish or Korean rockfish, *Sebastes Schlegeli*, is a well-known teleost species found on nearshore rocky bottoms at depths of 10-100 m. The main habitats of black rockfish consist of oceans around Korean peninsula, Japan and China. The habitats of the rockfish are usually the reef area of the shore. This fish grow to a maximum length of 40 cm. Black Rockfish is ranked the highest among marine fish in Korea as a game fish, and attracts millions of anglers all through the year (Yoon, Jong-Man ; Choi, Youn ; Kim 2007). The mass production of black rockfish was established in the early 1990s and currently it has become the second most cultivated fish in South Korea.

Fig. 1. The Black rockfish (*Sebastes Schlegel*i)

Proteases are widely distributed group of enzymes in all the living organisms, which play an indispensable role through catalyzing the hydrolysis process of peptides bonds of proteins at cellular level. According to the chemical group involve in the catalytic process, proteases can be categorized into five major groups, designated as serine, cysteine, aspartic, threonine and metallo proteases(Rawlings & Barrett 1999). Among them, cysteine proteases have been identified from almost all the taxonomic groups of organisms including prokaryotes, such as virus and bacteria showing a ubiquitous distribution (Rudenskaya & Pupov 2008). Processing of proteins by restricted cleavage is a crucial characteristic of cysteine proteases which in turn render them as role players in antigen presentation, photolytic processing of proenzymes and prohormones, fertilization, cell proliferation, differentiation and apoptosis in living creatures (Chapman et al. 1997). Cytosolic calpains and lysosomal cathepsins were identified as major groups of cysteine proteases in mammals (Turk et al. 2002), whereas papain is considered as a well characterized cysteine protease, having a plant origin (Jon 2012). All the cysteine proteases which show structurally close relationship with papain are categorized into a large single group known as papain family (Grzonka et al. 2001). Although, the function of proteases including cysteine proteases is an indeed necessity in organisms, their catalytic activity should be tightly regulated, since uncontrolled proteolysis can elicit deleterious consequences furnishing pathological conditions in living beings (Turk 2001; Turk et al. 2001) . In this regard, endogenous protein inhibition plays a substantial role as a key mechanism of regulating the catalytic activity of proteases.

Cystatins are large group of evolutionary related reversible inhibitors of cysteine proteases, which basically interact with papain family proteases including mammalian cathepsins, B, H and L (Turk & Bode 1991). Cystatins are known to inhibit the activity of target proteases by indirectly

obstructing the catalytic centers to prevent the docking and cleavage of the substrates (Bode & Huber 2000). Based on the size of polypeptide chain and the presence or absence of the disulphide bonds, cystatin super family has subdivided into three major families, family 1 known as stefins, family 2, known as cystatins and family 3, designated as kininogens (Josiah Ochieng & Gautam Chaudhuri 2010). Besides these three, novel proteases identified as cystatin family members shearing substantial sequence similarity with the existing cystatins, albeit lacking of cysteine protease inhibitory properties were categorized under a new family, called family 4 (Cornwall & Hsia 2003; Brown & Dziegielewska 1997).

Within the cystatin super family, family 1 cystatins, collectively known as stefins are represented by cystatin B and stefins A and B, which share the characteristic conserved regions important for the obstruction of the active site of C1 cysteine proteases, with other members; a glycine residue in the N-terminal region, a glutamine-valine-glycine (QxVxG) sequence which forms the part of a β-hairpin loop and C-terminal second hairpin loop consisted of proline-tryptophan (PW) residues (Turk & Bode 1991). 'Stefin' family members generally consist of ~ 100 residues and lack disulfide bonds or carbohydrates. The tertiary structure of stefins represents a typical 'cystatin fold' structure forming a central α helix, wrapped by a five–stranded β sheet (Stubbs et al. 1990; Bode et al. 1988).

On the basis of the higher inhibitory potential exert on cysteine proteases cystatins play several defensive roles and regulatory functions in different cellular events. For an instance, according to the recent studies, cystatins were found to induce the NO production through stimulation of TNF-α and IL-10 synthesis, which is a crucial defense strategy evoked upon pathogen infections (Verdot et al. 1996; Verdot et al. 1999). Moreover, teleostean cystatin Bs have also exhibited *in-vitro* antibacterial properties (Xiao et al. 2010). Although, molecular level studies

3

on different cystatin family members from higher vertebrate lineages have been carried out to date, detailed characterization of their lower vertebrate counterparts, reported abundantly, except from few species including *Oplegnathus fasciatus* (Premachandra, Whang, et al. 2012) and *Scophthalmus maximus* (Xiao et al. 2010).

Edible marine fish are considered as protein rich source in human diets, thus farming of fish has been cherished recently to compensate the increasing demand on them. However, as a consequence of intensive culturing of large scale of fish in restricted areas, different stress factors, more prominently pathogenic stress have adversely affected to the yield of worldwide fish mariculture farming, resulting considerable economic loss. Under the light of this background, investigations on molecular pathophysiology of mariculturable fish species can be considered as a primitive commencement of developing disease management strategies against the growing threat of pathogenic infections on them.

2. MATERIALS AND METHODOLOGY

2.1 Sequence identification and *In-silico* analysis

Based upon the alignments obtained from NCBI Genbank sequence database with our previously established black rockfish cDNA sequence database (Elvitigala et al. 2015) using Basic Local Alignment Tool (BLAST), a homolog of cystatin B sequences, designated as RfCytB was identified. Identified sequence was then used to demarcate the putative open reading frame (ORF) and subsequently derive the corresponding amino acid sequence by DNAsist 2.2 software package. Sequence comparison studies of predicted protein sequence with its homologs were performed using ClustalW2 program (multiple sequence alignment- (Thompson et al. 1994)) and Matgat software (pairwise sequence alignment-(Campanella et al. 2003)) programs. With the objective of investigating the evolutionary relationship with its counterpart molecules, phylogenic analysis of RfCytB was carried out using the Neighbor-joining method with bootstrapping values taken from 1000 replicates by Molecular evolutionary genetics Analysis (MEGA) software, version 6 (Tamura et al. 2013). Characteristic signatures of the RfCytB protein sequence were predicted by ExPASy-prosite server (http://prosite.expasy.org) and some of the physicochemical properties were identified using ExPASy ProtParam tool (http://web.expasy.org/protparam).

2.2 Preparations of *RfCytB* recombinant plasmid constructs

The coding sequence of the RfCytB was PCR amplified using corresponding oligomers designed with the compatible restriction enzyme sites (RfCytB-F, RfCytB-R) to the pMAL c2X plasmid vector (New England Biolabs, USA) or pCDNA™3.1/HisC (Table 1).The PCR was performed in a TaKaRa thermal cycler in a 50 µL total volume, containing 5 U of Ex Taq polymerase (TaKaRa, Japan), 5 µL of 10 X Ex Taq buffer, 8 µL of 2.5 mM dNTPs, 80 ng of

5

template and 10 pmol of each oligomer. The reaction was devised with an initial incubation at 94 °C for 4 min, followed by 35 cycles of 94 °C for 30 s, 55 °C for 30 s, and 72 °C for 45 s, and a final extension at 72 °C for 3 min. Subsequently, the pMAL-c2X vector and amplified products were digested with respective restriction enzymes and analyzed by gel electrophoresis. Fragments matched with the expected size were excised, purified using the Accuprep gel purification kit (Bioneer Co., Korea) and ligated into pMAL-c2X by Overnight incubation with Mighty Mix (TaKaRa) at 4 °C to prepare the pMAL-c2X/*RfCytB* fusion construct. On following day the ligated product was transformed into *Escherichia coli* (*E. coli*) DH5α cells. Finally, the cloned coding region of RfCytB was confirmed by sequencing at Macrogen-Korea.

2.3 Over expression and purification of recombinant RfCytB

RfCytB recombinant fusion constructs were transformed into *E.coli* BL21 (DE3) competent cells and the respective putative single colonies bearing the constructs contained the deleted and complete coding regions were selected. Then the selected colonies were separately grown overnight in a 500 mL LB broth medium, supplemented with 100 µg/mL ampicillin at 37 °C with shaking (200 rpm). After the optical density (OD) at 600 nm reached to 0.6, isopropyl-β-thiogalactopyranoside (IPTG) was mixed at a final concentration of 0.5 mM and the final mixture was incubated for 8 h at 20 °C to induce recombinant protein expression. Subsequently, cells were cooled on ice for 30 min and harvested by centrifugation at 3500 rpm for 30 min at 4 °C. The obtained pellets were resuspended in column buffer (20 mM Tris-HCl, pH 7.4 and 200 mM NaCl) and stored at – 20 °C overnight. On the following day, cells were thawed at chilled conditions and ruptured by cold sonication in the presence of lysozyme (1mg/mL) and the resultant solution was separated by centrifugation (9000 g for 30 min at 4 °C). The supernatant was defined as crude extract and the recombinant proteins (complete and deleted products) were purified using pMAL

protein fusion and purification technique (New England BioLabsInc, USA). Subsequently, the concentration of the purified fusion protein products were determined using Bradford method and rRfCytB-MBP fusion product was cleaved using Factor Xa, according to the pMAL™ Protein Fusion and Purification kit protocol to use the resultant cleaved protein product mixture (rRfCytB) for functional assays. Then, the samples collected at different steps of the rRfCytB purification were analyzed using 12 % SDS-PAGE under reduced conditions using standard protein size markers (Enzynomics, Korea), confirming the sufficient purity along with integrity of the fusion protein and its successful cleavage by factor Xa.

Table 1 Oligomers used in the study of RfCytB

Name	Application	Sequence (5′ →3′)
RfCytB-qL	qPCR of *RfCytB*	GAGGATCACGTTCACCTCCGTGTTTA
RfCytB-qR	qPCR of *RfCytB*	CAATCTCGTCATCGGAGGACTTGGA
RfEF1A-F	qPCR of *RfCytB*	AACCTGACCACTGAGGTGAAGTCTG
RfEF1A-R	qPCR of *RfCytB*	TCCTTGACGGACACGTTCTTGATGTT
RfCytB -CL	Cloning for pMAL-c2x	GAGAGAgaattcATGATGTGTGGAGGGATTGGA GAAGTTAAG
RfCytB -CR	Cloning for pMAL-c2x	GAGAGAaagcttTTAGAAGTACTCAATCTCGTC ATCGGAGGA
RfCytB -TL	Cloning for pcDNA3.1/HisC	GAGAGAgaattcgtgatggggaATGATGTGTGGAGGG ATTGGAGAAGTTAAG
RfCytB -TR	Cloning for pcDNA3.1/HisC	GAGAGActcgagTTAGAAGTACTCAATCTCGTC ATCGGAGGA

2.4 Papain inhibitory activity assay

Cysteine protease inhibitory activity of rRfCytB was evaluated against crude papain (P3375; Sigma-Aldrich, St, Louis, MO, USA) according to a previously published method with some modifications. Briefly, crude papain was dissolved in potassium phosphate buffer (PPB; pH-7.6) to reach the final concentration of 1mg/mL and then mixed each 10 µL of the solution with different volumes of rRfCytB to meet 0/1 (negative control) 1/8, 1/4, 1/2, 1, 2, 3, 4, 5 rRfCytB/papain concentration ratios in a final PPB volume of 120 µL. Subsequently, mixture was incubated at 25 ℃ for 15 min and 50 µL of azo casine (0.5 %) was added to the each mixture and then incubated at 37 ℃ for 20 min, after proper mixing. Thereafter, the reaction was terminated by adding 100 µL of 10 % trichloroacetic acid to the final reaction mixtures. Finally, the mixtures were centrifuged and the supernatant was used for OD measurements at 440 nm. One control experiment was carried out using equal amount of elution buffer (column buffer + 10mM maltose) instead of the protein. Another control experiment was also carried out using MBP treated with factor Xa (MBP/papain concentration ratio = 5) instead of rRfCytB following the same experimental procedure to investigate the effect of MBP on the activity in cleaved rRfCytB. The relative inhibitory activity was calculated using 100 x [1- (OD_{440} of protein treated sample/ OD_{440} of negative control)]. All the assays were triplicated and data were presented as the mean of the repeated assays. Moreover, the experiment was repeated using 4:1 rRfCytB/papain ratio after heating the rRfCytB protein at 90 ℃ for 0, 10, 20, 30, 40 , 50, 60 min, respectively to assess the thermal stability of the protein using triplicated assays.

2.5 Construction of expression vector and transfection assay

2.5.1 Construction of expression vector

The full-length CDS of RfCytB (294 bp) was PCR amplified from gill cDNA using gene specific primers (Table 1) and then sub cloned into pCDNA^{TM} 3.1/HisC (Life Technologies). The clone harboring the RfCytB CDS was affirmed by sequencing and termed as pcDNA-RfCytB.

2.5.2 Cell Culture and Transfection

Murine Macrophage cells were grown in Dulbecco Modified Eagle Medium (DMEM-WELGENE-Korea) supplemented with 10% fetal bovine serum (FBS) and maintained at 37°C in 5% CO_2. The prepared pcDNA-RfCytB recombinant construct was transiently transfected into Murine Macrophage cells using the X-tremeGENE™ 9 DNA Transfection Reagent (Roche, USA), according to manufacturer's instructions. After the transfection, over-expression of RfCytB was confirmed by a qPCR assay conducted on transfected, mock controls (empty pCDNA3.1/HisC) and transfection controls (without vector) by comparing the expression level with the un-transfected control. Murine beta actin gene was used as the internal control (GenBank ID: AAI38615) and corresponding primer pair (Table 1) for RfCytB was used for the qPCR. The transfected cell lines were treated with LPS at 24 h after the transfection to activate and induce inflammatory conditions in cells and analysed the expressional modulation of TNFα and iNOS genes after 24 h post treatment by qPCR with corresponding primer pairs (Table 1) and using murine beta actin gene as an internal control. Details on reaction conditions and reagents of aforementioned qPCR assays are identical to the details mentioned in section 2.9. In order to confirm the success of transfection and to further analyse the downstream gene expression, the expression level of transfected RfCytB was assessed by qPCR at 48 h p.i.

제주대학교 중앙도서관
JEJU NATIONAL UNIVERSITY LIBRARY

2.6 Animal rearing and tissue collection

Healthy fish acclimatized to the laboratory conditions were obtained from one of the aquariums in Marine Science Institute of Jeju National University, Jeju Self Governing province, Republic of Korea and maintained in 400 L laboratory aquarium tanks filled with aerated seawater at $18 \pm 1°C$. Five healthy fish with average body weight of ~ 35 g were sacrificed for the tissue collection. Before scarification, ~ 1 mL of blood was collected from each fish using sterile syringes coated with 0.2 % heparin sodium salt (USB, USA) and the peripheral blood cells were separated by immediate centrifugation at $3,000 \times g$ for 10 min at 4 °C. Other tissues including head kidney, spleen, liver, gill, intestine, kidney, brain, muscle, skin and heart were excised and snap-frozen in liquid nitrogen and stored at −80 °C.

2.7 Immune challenge experiments

In order to investigate the modulatory properties of atypical *Aeromonas salmonocida* infection on RfCytB transcription, which is a known gram negative bacterial threat in black rockfish aquaculture (Han et al. 2011), healthy fish acclimatized to the laboratory conditions were intraperitoneally injected with 100 µL of live *A. salmonocida* (RFAS-1 strain - 1×10^9 CFU/mL), according to the pre-determined sub-lethal dose of the reared fish, in sterilized phosphate buffered saline (PBS). For the injection control group, fish were injected with 100 µL PBS. Head kidney and spleen tissues of the experimental animals were collected as described in section 2.6 sacrificing at least five animals at 6, 12, 24, 48, 72 and 120 h post-injection.

2.8 Total RNA extraction and cDNA synthesis

Total RNA was extracted from pool of each excised tissue of five healthy fish whereas head kidney and spleen tissues from five immune challenged or PBS injected fish corresponding

10

to each time point, using the RNAiso plus[TM] (TaKaRa, Japan) reagent according to the vendor's protocol. Tissue pooling was carried out as follows; 660 mg of brain tissues, ~50 mg of kidney tissues (~10 mg from each fish), ~125 mg of heart tissues (25 mg of each) and ~150 mg of all the other tissues (30 mg of each). Concentration of extracted RNA from different tissues was determined at 260 nm in a UV-spectrophotometer (Thermo scientific, USA) and diluted to 1 µg/µL. Portion of 2.5 µg of RNA from selected tissues was applied in cDNA synthesis using a cDNA synthesis kit (TaKaRa, Japan) according to the manufacturer's instructions. Finally, this newly synthesized cDNA was 40 fold diluted (total 800 µL) and stored at -20 °C until for further analysis.

2.9 RfCytB transcriptional analysis by quantitative real time PCR (qPCR)

The mRNA expression level of RfCytB was investigated in the tissues mentioned in section 2.6 and the temporal expression of RfCytB in spleen and head kidney tissues. After total RNA extraction followed by cDNA synthesis, qPCR was carried out using the thermal cycler Dice[TM] real time System (TP800; TaKaRa, Japan) in a 10 µL reaction volume containing 3 µL of diluted cDNA from corresponding tissue, 5 µL of 2x TaKaRa Ex Taq[TM], SYBR premix, 0.4 µL of each primer (RfCytB-qF and RfCytB-qR; Table 1), and 1.6 µL of dd H_2O. The qPCR was performed under the following conditions: 95 °C for 10 s, followed by 40 cycles of 95 °C for 5 s, 58 °C for 10 s and 72 °C for 20 s and the final cycle of 95 °C for 15 s, 60 °C for 30 s and 95 °C for 15 s. The base line was set automatically by Dice[TM] Real Time System software (version 2.00). RfCytB expression level was determined by the Livak ($2^{-\Delta\Delta CT}$) method (Livak & Schmittgen 2001). The same qPCR cycle profile was used for the internal control gene, black rock fish elongation factor α (RfEF1A; GenBank ID: KF430623). All data are represented as means ± standard deviation (SD) of relative mRNA expression of triplicates, further compared to the respective expression folds of RfEF1A gene. Moreover, the temporal expression folds of RfCytB detected for the immune

11

challenged groups were normalized to the corresponding expression levels of PBS injected controls, considering the plausible effect of the medium of injection. To determine the statistical significance ($P < 0.05$) between the experimental and control groups, two tailed T-test was carried out.

3. RESULTS AND DISCUSSION

3.1 Sequence characterization and phylogenetic position

A homologues DNA sequence (573 bp) to the known cystatin B counterparts was identified from our black rockfish cDNA database and designated as *RfCytB*. Complete putative ORF of *RfCytB* was 291 bp in length which encodes for a protein of 97 amino acids with a predicted molecular mass of 11 kDa and theoretical iso-electric point of 6.3. The protein sequence resembles the conserved cystatin family signature including single cystatin like domain, cysteine protease inhibitory signature (residues ^{46}QLVSGTNYFIKVH^{58}) harboring pantapeptide QXVXG consensus sequence which is located on hairpin loop of the protein and N-terminal two conserved neighboring glycine (^{8}GG^{9}) residues (Fig. 2). Two G residues are known to constitute a wedge shape edge involving in inhibition of protease activity, which is complementary to the active site of the papain like cysteine proteases (Turk & Bode 1991; Bode et al. 1988). Moreover, variant of typical cystatin family c-terminal proline-tryptophan (PW) motif was also identified in RfCytB, where tryptophan residue was replaced by a cysteine (C) residue. Such variations were also reported previously with diverse cystatin B counterparts; for instance, tryptophan residue of PW motif of human stefin B was replaced by histidine (H) residue (Manuscript & Superfamily 2011).

```
Black Rockfish     --MMCGGIGEVKDANEEVHKICESVKPHAEKQAGKTFDVFTAKTYKTQLVSGTNYFIKVH 58
Turbot             -MPLCGGLGESANADDDIQKICDSMKPHAEEKTGKSFAVFTAKTYKTQLVSGTNYFIKVH 59
Rock bream         MSMMCGGISAPLDADEDIQKMCDNVKPHAEEKAGKKYDVFTAKTYTTQIVSGTNYFIKIH 60
European seabass   MSMMCGGLNEPIDADDKIHKICETLKPHAEQRAGKTFEVFTAKSYSTQVVAGTNYFIKVH 60
Olive flounder     --MLCGGTSQPVDADEQIQKICDSMKPHAEAQAGKTFDVFVAKTYTTQCVPGTNYFIKVH 58
Human              --MMCGAPSATQPATAETQHIADQVRSQLEEKENKKFPVFKAVSFKSQVVAGTNYFIKVH 58
Mouse              --MMCGAPSATMPATAETQEVADQVKSQLESKENQKFDVFKAISFKRQIVAGTNLFIKVD 58
                     :**. .      *    . :.:.: ::.: * : .:.: ** * ::. * *.*** ***:.


Black Rockfish     VGGEDHVHLRVYKPLPCNG-EIQLSKMQHSKSSDDEIEYF 97
Turbot             VGEEEHLHIRVYKKLQCNGGEIELTSLQENKSHHDPIVYF 99
Rock bream         VGGDDHVHLRVYKKLPCHGGGLELSGMQHSKSLQDPIAYF 100
European seabass   VGGDDHVHLRVYEKLPCHGGDLELSAMQQSKSHQDPIEYF 100
Olive flounder     VGGDEHVHLRVYKKLPCNGETLELSKMLQDKRHHDPLEYF 98
Human              VGDEDFVHLRVFQSLPHENKPLTLSNYQTNKAKHDELTYF 98
Mouse              VGGDKCVHLRVFQPLPHENKPLTLSSYQTNKERHDELSYF 98
                   ** :. :*:**:: *  .. : *:    .*  .* : **
```

Fig. 2. Multiple protein sequence alignment of vertebrate cystatin B counterparts including black rockfish cystatin B (RfCytB). Completely conserved and partially conserved residues were denoted by (*) and (: or .) symbols respectively. N-terminal two conserved neighboring glycine (G) residues and conserved Q,V and G residues in consensus QxVxG pentapeptide sequence in cysteine protease inhibitory signature (indicated by double headed arrow) were shaded in gray color. The variant of typical cystatin family c-terminal proline-tryptophan (PW) motif (PC) was underlined on RfCytB protein sequence and the putative motifs corresponding to other sequences were boxed.

According to our pairwise sequence alignment study, RfCytB shared significant sequence compatibility with its teleostean cystatin B counterparts with the eminent similarity (82.7 %) and identity (68.4 %) with olive flounder cystatin B validating its homology to cystatin B counterparts (Table 2).

Table 2 Percentage similarity and identity values of RfCytB with different cystatin homologues.

No.	Name of the species	Protein	GenBank accession Number	Amino acids	Identity (%)	Similarity (%)
1	*Paralichthys olivaceus* (Olive flounder*)*	Cystatin-B	ACC86114	98	68.4	**82.7**
2	*Oplegnathus fasciatus* (Rock bream)	Cystatin-B	AFP50145	100	68	**84**
3	*Dicentrarchus labrax* (European seabass)	Cystatin-B	CBN81974	100	68	**88**
4	*Salmo salar* (Atlantic salmon)	Cystatin-B	ACI66582	99	66.7	**81.8**
5	*Scophthalmus maximus* (Turbot)	Cystatin-B	ADM61584	99	64.6	**84.8**
6	*Danio rerio* (Zebrafish)	Cystatin-B	NP001096599	100	64	**81**
7	*Gallus gallus* (Chicken)	Cystatin-B	NP001185577	98	51	**72.4**
8	*Homo sapiens* (Human)	Cystatin-B	NP000091	98	46.9	**65.3**
9	*Rattus norvegicus* (Rat)	Cystatin-B	NP036970	98	45.9	**63.3**
10	*Mus musculus* (Mouse)	Cystatin B	NP031819	98	44.9	**62.2**
11	*Homo sapiens* (Human)	Cystatin-A	NP005204	98	41.8	**65.3**
12	*Mus musculus* (Mouse)	Cystatin-A	NP001028411	97	40.2	**66**
13	*Rattus norvegicus* (Rat)	Cystatin A	NP001099346	97	40.2	**64.9**
14	*Bos taurus* (Bovine)	Cystatin A	NP001161296	98	39.8	**65.3**
15	*Mus musculus* (Mouse)	Cystatin C	AAA63298	140	19.7	**32.1**
16	*Onchocerca volvulus*	CPI	P22085	162	16.2	**30.9**
17	*Rattus norvegicus* (Rat)	Cystatin C	NP036969	140	16.2	**32.1**
18	*Bos taurus* (Bovine)	Cystatin C	NP776454	148	15	**32.4**
19	*Homo sapiens* (Human)	Cystatin C	NP_000090	146	14.9	**31.5**
20	*Saimiri sciureus* (Monkey)	Cystatin C	O19093	146	14.8	**28.1**
21	*Acanthocheilonema viteae* (Rodent filaria worm)	Cystatin	AAA87228	157	14.6	**31.2**
22	*Brugia malayi* (Filaria nemotode worm)	CPI-2	AAD51086	161	14.3	**29.8**
23	*Homo sapiens* (Human)	Cystatin D	CAA49838	142	13.9	**27.5**
24	*Mus musculus* (Mouse)	Kininogen	NP075614	432	9	**15.7**
25	*Homo sapiens* (Human)	Kininogen	NP000884	427	8.7	**12.9**
26	*Bos taurus* (Bovine)	Kininogen	NP001106748	619	6.8	**10.5**
27	*Rattus norvegicus* (Rat)	Kininogen	NP036873	639	6.3	**9.1**

Our phylogenetic reconstruction separates different vertebrate and invertebrate cystatin counterparts into closely and independently clustered clades corresponding to known four different cystatin families accordingly, in which RfCytB was clustered into family 1, showing closer evolutionary relationship with its teleostean cyststin B counterparts, as expected (Fig. 3).
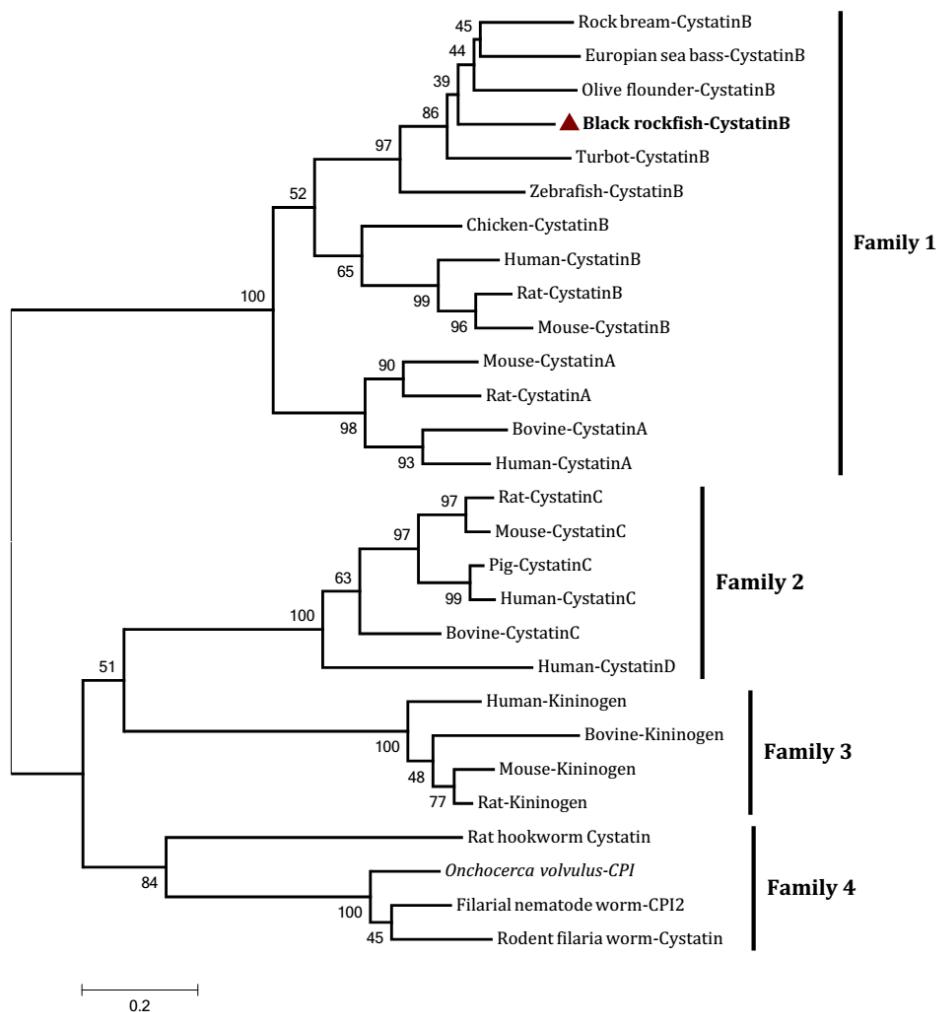

Fig. 3. Phylogenetic position of RfCytB analyzed by MEGA version 6.0 software based on ClustalW2 multiple sequence alignment of different vertebrates and invertebrate counterparts under the neighbor-joining platform. Bootstrap supporting values are denoted at the tree branches and NCBI-GenBank accession numbers of used cystatin homologues are mentioned in Table 2.

According to the tree topology of teleostean cystatin B counterparts, exclusively Rock bream and European sea bass cystatin Bs were clustered in a close and independent clade whereas in accordance with the order, olive flounder, black rock fish, turbot and zebrafish counterparts were clustered with increasing phylogenetic distance with that clade. As expected Cystatin B and as were clustered separately under family 1 cystatins, whereas, family 2, 3 and 4 counterparts were clustered closely and independent to each other group. Moreover, family 1 cystatins showed phylogenetically distance relationship with rest of the cystatin family members, originating from a separate ancestor. On the other hand, family 2, 3 and 4 members shared common ancestral origin where family 2 and family 3 members exhibited relatively closer evolutionary relationship. Collectively, deciphered phylogenetic relationship of RbCytB with different cystatin family similitudes clearly asserts its homology with teleostean cystatin Bs and its vertebrate ancestral origin.

3.2 Papain inhibitory activity of rRfCytB

Cystatins are known as potent inhibitors of papain family proteases (Turk & Bode 1991) and some of the vertebrate and invertebrate cystatin B counterparts were shown to have detectable papain inhibitory activity. For instance, disk abalone (Premachandra, Wan, et al. 2012), manila clam (Premachandra et al. 2013) counterparts with invertebrate origin and rock bream (Premachandra, Whang, et al. 2012) and turbot (Xiao et al. 2010) counterparts with vertebrate origin have demonstrated concentration depended papain inhibitory activity. Thus, we intend to investigate the potential papain inhibitory activity of rRfCytB using different papain: rRfCytB ratios. According to the results, with the increasing concentration of rRfCytB (with higher papain: rRfCytB ratios) inhibitory activity was detected to elevate, as expected (Fig. 4). The highest activity (76 %) was noted with 1:5 papain: rRfCytB concentration ratio. In contrast, in study on

17

manila clam cystatin B, the maximum inhibition (~80 %) was noted for the 1:1 papain: rRfCytB concentration ratio. This comparison may reflect the lesser efficiency of rRfCytB in cysteine protease inhibition, compared to its invertebrate's counterparts. As expected, MBP treated control did not show any significant papain inhibitory activity (~ 8 %) compared to the rRfCytB treated experiments up to 4:1 papain: rRfCytB concentration ratio, suggesting the negligible interference of the MBP in the fusion rRfCytB. Taken together these results infer the putative dose dependent cysteine protease inhibitory activity of rRfCytB.

Papain Inhibitory Activity
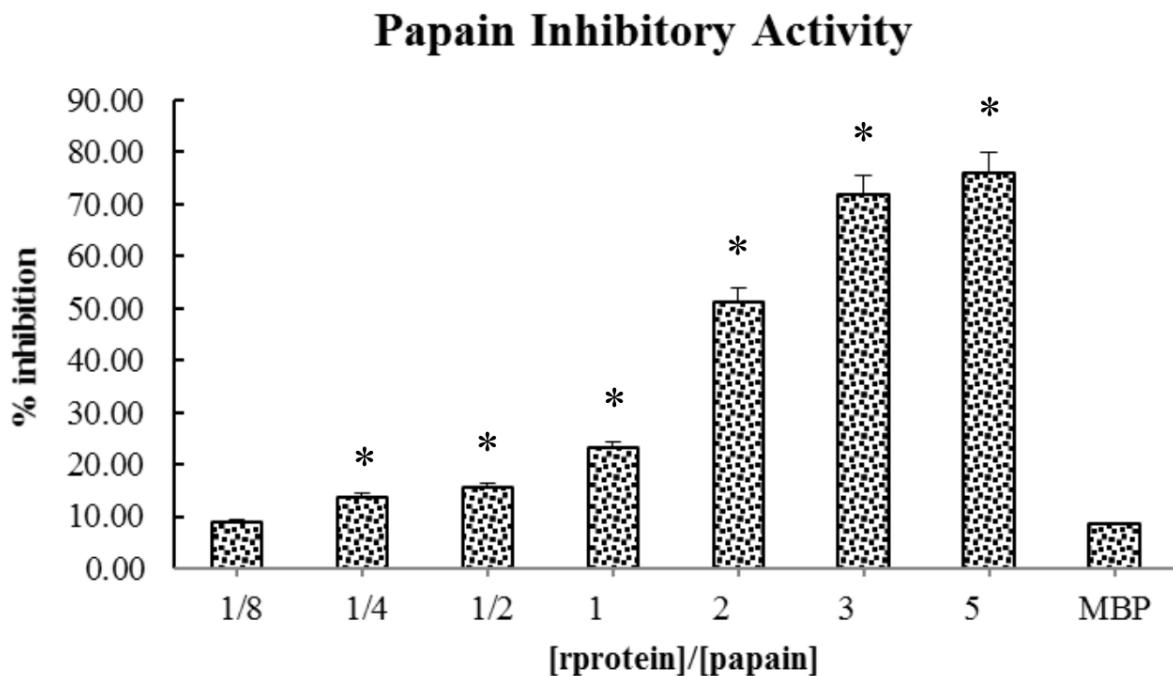
Fig. 4. In-vitro papain inhibitory activity at different concentrations of rRfCytB. Azo-casein was used as the substrate of papain enzyme and MBP was used as a control. Error bars represent SDs (n =3) and each asterisk indicates the significant differences (P<0.05) compared to the % inhibition of MBP treated control, obtained from the t test.

3.3 Thermal stability of rRfCytB

We investigated the thermal stability of rRfCytB fusion protein by monitoring its papain inhibitory activity after heating the recombinant protein in time course manner. Intriguingly, rRfCytB demonstrated significant thermal stability, showing marked papain inhibitory activity (80 – 90 %) after heating the rRfCytB for different time periods (Fig. 5). Even after, 60 min of heating, recombinant protein demonstrated a ~ 83 % relative residual inhibitory activity, which is exclusively exhibiting a significantly lower ($p < 0.05$) activity compared to the activity detected for un-heated control. It was reported that cystatins do not form covalent bonds with cysteine proteases; hence does not tightly interact with the proteases. On the other hand, they can cover the active site cleft to obstruct the access of the relevant substrate to the active site of the proteases (P.A. Pemberton 2006). Therefore, the structural damages elicit by environmental factors like high temperatures on cystatins may not severely alter its cysteine protease inhibitory activity, agreeing with what we observed herein regarding rRfCytB. However, showing an contrasting outcomes to what we have observed, expressed recombinant cystatin counterpart of Chinese sturgeon was found to lose its papain inhibitory activity with heating even at 70 ℃ in time course experiment, initially with high rate and later low rate of papain inhibitory activity reduction with the time, up to 40 % of initial activity (after 60 min of heating) with unheated control (Bai et al. 2006).
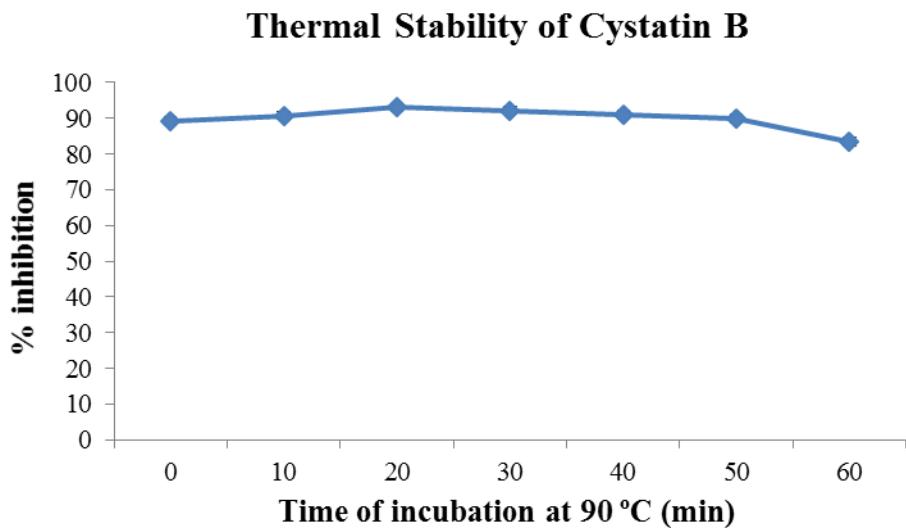
Fig. 5. Thermal stability of RfCytB with time, by monitoring its papain inhibitory activity after heating the recombinant protein in time course manner.

3.3 Transfection of rRfCytB

The transfection study, conducted to observe the modulation of maker genes of an inflammatory condition in murine macrophages upon the over-expression of cystatin B displayed positive results from the subsequent qPCR analysis. The transcription level of *RfCytB* was extremely higher than the control cells bringing to a conclusion that the RfCytB was overproduced in transfectants, thus confirming the overexpression of *RfCytB* in murine macrophages (Fig. 6A). Further analysis of immune related genes associated with inflammatory conditions with the Cystatin B overexpression displayed increased expression of *iNOS* and *TNF-α* (Fig. 6B). Cystatin B and other two cystatins are known to up-regulate the release of Nitric oxide (NO) from activated macrophages (Hartmann et al. 2002; Marletta 1993). Previous studies have certified the pathway of up-regulation of NO release is merely upon the synthesis of TNF-α and IL-10 (Josiah Ochieng & Gautam Chaudhuri 2010). The achieved results proves itself the relation between the up-

20

regulation of CytB, TNF-α and iNOS. These findings further ascertain the importance of cystatin B in teleost innate immune system related to bacterial infection.
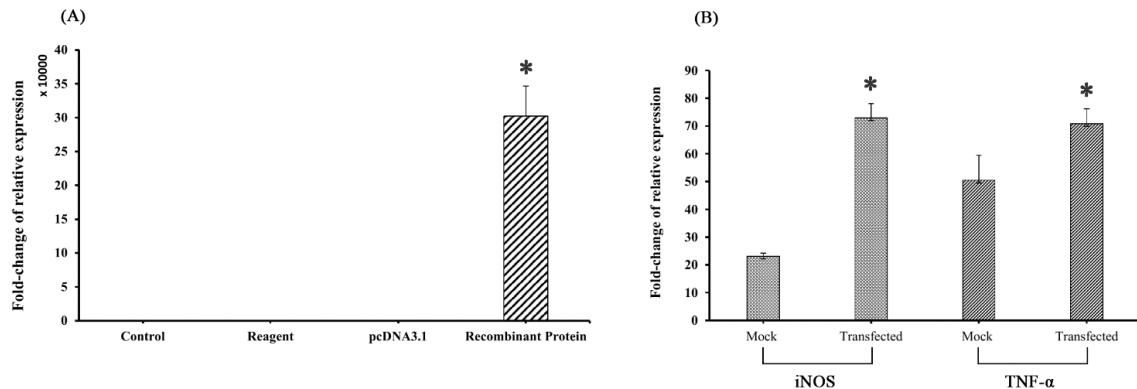
Fig. 6. Gene expression analysis of transfection study by qPCR. The empty pcDNA3.1 vector and pcDNA3.1-RfCytB were transfected into murine macrophage cells. After 24 h of transfection the cells were treated with LPS and then the cells were harvested after 24 h. RNA was isolated, cDNA was prepared and gene expression was analyzed by qPCR. The expression was normalized to Beta-actin to mock controls. **(A)** rRfCytB Gene expression in control (Without any treatment), transfection reagent treated control, mock control and the transfected cells. **(B)** Expression patterns of iNOS and TNF-α genes post transfection in pcDNA3.1-RfCytB transfected cells and corresponding mock controls. Error bars represent SDs (n =3) and each asterisk indicates the significant differences (P < 0.05) obtained from t test.

3.4 Tissue specific mRNA expression

According to the outcomes of our qPCR assay, *RfCytB* was detected to be ubiquitously expressed in tissues examined, albeit with different folds (Fig. 7.).
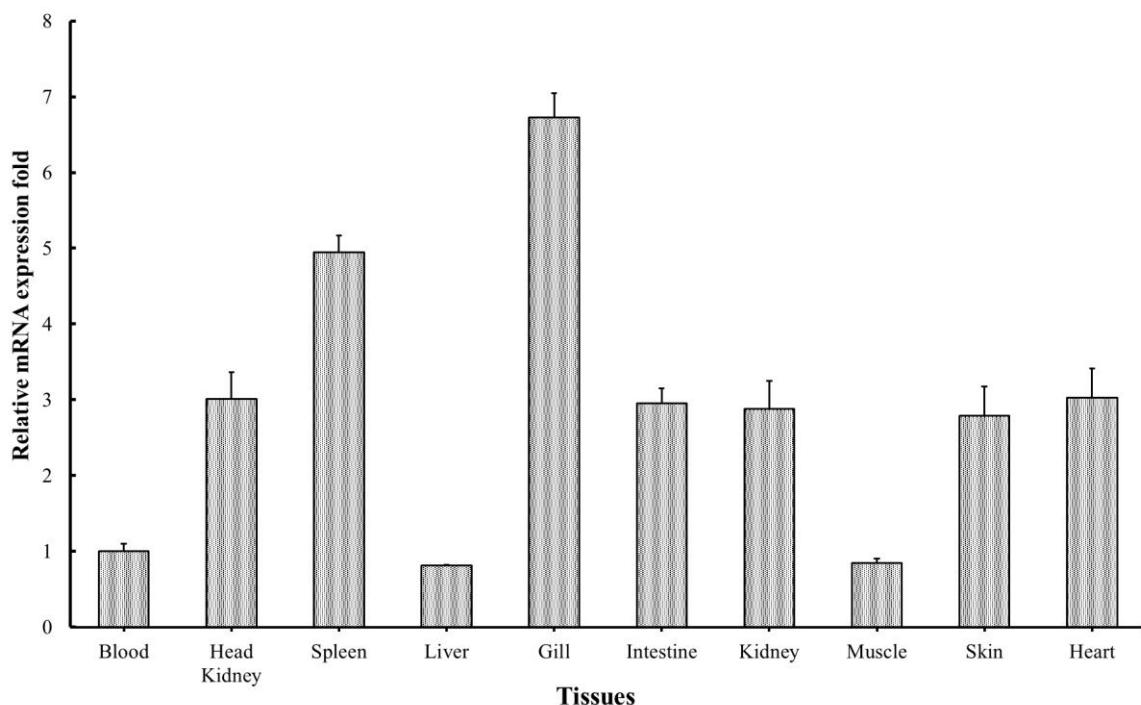
Fig. 7. Spatial expression of RfCytB was determined by quantitative real-time PCR in different tissues of unchallenged black rockfish. The Livak method was used to determine relative mRNA expression, and the elongation factor-1α of black rockfish was used as a reference gene. Vertical bars represent the SD.

Expression was pronouncedly detected in gill and spleen tissues, whereas least expression levels were observed in muscle and liver tissues. Gills are frequently in contact with outer environment; thus more vulnerable for pathogen infections. Cystatins including cystatin B are involved in disease pathology in addition to normal proteolysis process, in which they are known

to modulate the immune responses against invading pathogens (Zavasnik-Bergant 2008). Hence, it is likely to expect a pronounced level of RfCytB expression in gill tissues which may involve in inhibition of crucial cysteine proteases in pathogens like bacteria, virus or parasites to suppress their proliferation and survival in host cells. Spleen of teleost's is the largest lymphoid organ which harbors essential cellular components of innate immunity including aggregates of macrophages (melanomacrophages) (Zapata et al. 2006; Uribe et al. 2011). On the other hand teleostean cystatin Bs were shown to have antimicrobial effect in teleostean macrophages (Xiao et al. 2010) and up-regulate the nitric oxide (NO) release from IFN-γ activated murine macrophages (Verdot et al. 1996; Hartmann et al. 2002). Thus, it is logical to assume that RfCytBs are expected to be highly expressed even in spleen tissues to partake in aforementioned immune functions of melanomacrophages.

Complying with tissue specific expression of RfCytB, olive flounder cystatin B was detected to express ubiquitously in selected tissues examined with prominent expression in gill tissues (Ahn et al. 2013). Moreover, manila clam cystatin B was reported to express in all tissues tested with pronounced mRNA expression levels in hemocytes as well as gill tissues (Premachandra et al. 2013). However, contrasting with RfCytB tissue expression, turbot cystatin B mRNA was found to express abundantly in muscle tissues and weakly in spleen, blood gill and kidney tissues. On the other hand, within the detected universal tissue specific transcriptional profile of rock bream cystatin B, liver tissues showed eminent mRNA expression followed by the tissues of spleen and gill, brain and intestine (Premachandra, Whang, et al. 2012). However, muscle showed least abundant cystatin B mRNA expression in rock bream consistent with our observation on RfCytB tissue specific transcription.

3.5 Transcriptional response to the experimental pathogen infection

In order to prefigure the potential importance of RfCytB on host immune responses, we sought to decipher its temporal transcriptional responses to experimental infection with known pathogen of black rockfish; *A. salmonocida*. As detected by our qPCR assays, significant modulation of *RfCytB* was noted in spleen as well as head kidney tissues in response to the live bacterial infection. Upon the infection, mRNA expression of RfCytB was up-regulated in spleen tissues with ~ 3.4 fold compared to its basal level (0 h post infection (p.i.)) at 12 h p.i. with a significant ($P < 0.05$) down-regulation at 3 h p.i (Fig. 8A). The initial expressional reduction in spleen may reflect an mRNA turn-over event under pathogenic stress conditions. Interestingly, head kidney showed noticeable transcriptional modulation exclusively with inductive transcriptional responses against the infection at early, middle as well as late phase p.i. (6 h, 12 h and 48 h p.i.), in which more pronounced fold increase (~ 45 fold) was observed at 12 h p.i. compared to the basal level (Fig. 8B). However, in comparison with the transcriptional responses of head kidney and spleen, marked modulation of RfCytB could be observed in head kidney than spleen, compared to its basal level expression. Both teleostean head kidneys and spleens are enriched with macrophages aggregating into melanomacrophage centers (Uribe et al. 2011). As cystatins are known to involve in antimicrobial defense in teleostean macrophages, it can be assumed that overexpression of cystatins is expected upon a pathogen infection to involve in host immune responses eliciting pathogen clearance. Taken together, detected transcriptional responses of RfCytB against our bacterial infection suggest its putative importance in host antibacterial defense.
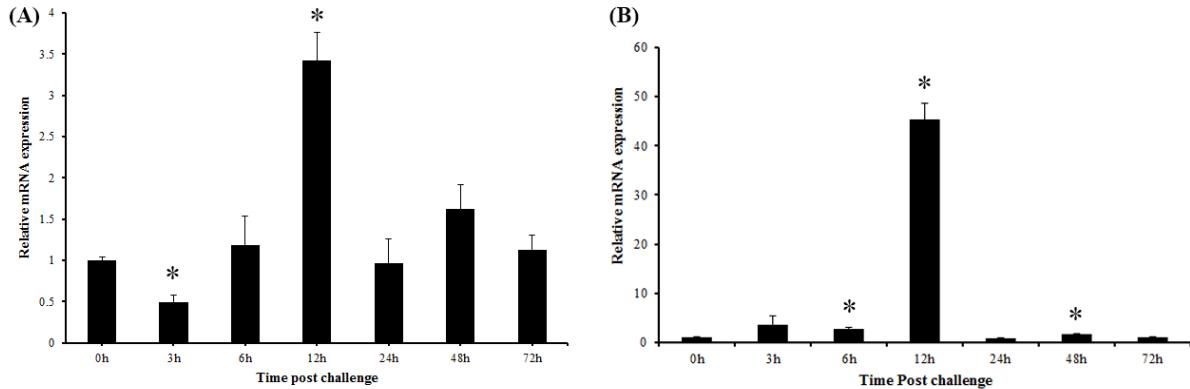
Fig. 8. The temporal mRNA expression of RfCytB in spleen **(A)** and head kidney **(B)** rock fish tissues after A. salmonocida injection detected by SYBR green qPCR. The relative expression was calculated using the $2^{-\Delta\Delta CT}$ method using black rock fish elongation factor α as the internal reference gene. All values were normalized to corresponding PBS-injected controls at each time point. The relative fold-change in expression at 0 h post-injection was used as the baseline. Error bars represent ±SD (n = 3), and each asterisk indicates the significant differences (P<0.05).

Complying with our outcomes of the experimental challenge experiment, rock bream cystatin was reported to elevate its mRNA expression level post *in-vivo Edwardsiella tarda* treatment in head kidney and spleen tissues with marked fold increase in head kidney tissues (Premachandra, Wan, et al. 2012). Moreover, same stimulus could trigger inductive transcriptional responses of turbot cystatin B gene in kidney, spleen, and brain and liver tissues within 24 h p.i. (Xiao et al. 2010). In contrast, as reported previously olive flounder cystatin B was not significantly induced upon the treatment with well-known bacterial endotoxin; lipopolysaccharide in kidney and gill tissues, but with slight inductions in muscle and spleen tissues at 24 h post treatment (Ahn et al. 2013).

4. CONCLUSION

In conclusion, the current study identified and functionally characterized Cystatin B from Korean black rockfish. Cystatin B was evolutionary conserved from fish to mammals. It was ubiquitously expressed in different tissues and the expression fluctuates upon bacterial simulation. Moreover, over-expression of RfCytB could trigger the up-regulation of pro-inflammatory genes in murine macrophages. Collectively, these findings on rockfish Cystatin B provide evidences in understanding the role of Cystatin B in fish lineages and the immunological importance to host defense.

CHAPTER 2

1. INTRODUCTION

In biological systems, the formation and overproduction of reactive oxygen species (ROS) are generated by a varied range of environmental factors and as byproducts of oxidative metabolism (Valko et al. 2006; Nordberg & Arnér 2001). Slight amounts of ROS are required for signaling pathways and in regulation with a variety of cellular activities and gene expression (D'Autréaux & Toledano 2007). However, excessive levels of ROS may increase the oxidative damage in cells by altering or inactivating proteins, lipid membranes and DNA (Hensley et al. 2000). To prevent such a phenomena, reactions involving antioxidants have shown to counterbalance the accumulations of ROS, thus mediating their harmful effects (Seifried et al. 2007). Antioxidants function primarily as molecular components to inhibit the oxidation of other molecules by ROS (Birben et al. 2012). Interdependent antioxidant systems are present in organisms to defend against oxidative injury. Glutathione peroxidase, glutathione reductase, glutaredoxin, catalase and superoxide dismutase are the enzymes that participate in counteracting with the ROS (Rudneva 1999).

Glutaredoxins (GLRX) are small ubiquitous oxidoreductases that belong to the thioredoxin (Trx) superfamily and which contain a CxxC/S active site motif (Vlamis-Gardikas & Holmgren 2002). Glutaredoxins can be categorized into 3 groups. The first group contains the classical GLRXs of about 9-14 kDa with two cysteines in their active sites. The second group mainly consists of the monothiol GLRXs which lacks a C terminal, and the third corresponds to a very particular type of glutaredoxin presenting more homologies with glutathione-S-transferase (GST) than with other GLRXs (Vlamis-Gardikas & Holmgren 2002; Lillig et al. 2005; Rodríguez-

Manzaneque et al. 1999; Vlamis-Gardikas et al. 1997). Glutaredoxin system consists of NADPH, glutathione reductase (GR), glutathione (GSH) and glutaredoxin (GLRX). All redox proteins belonging to the thioredoxin and glutaredoxin systems exist as isoenzymes, where Trx1, TrxR1 and GLRX1 are mainly cytosolic, and Trx2, TrxR2 and GLRX2 predominantly localize to the mitochondria (Gromer et al. 2004; Lillig et al. 2008). Both Glutaredoxin and Thioredoxin redox systems are involved in several important biological functions such as apoptosis, defense against oxidative stress, synthesis of DNA, thiol redox control of enzymes, as well as regulation of receptors and transcription factor (Lillig & Holmgren 2007). The major function of GLRX act in antioxidant defense by reducing dehydroascorbate, peroxiredoxins, and methionine sulfoxide reductase. Beside their function in antioxidant defense, bacterial and plant GRX were shown to bind iron-sulfur clusters and to deliver the cluster to enzymes on demand (Rouhier et al. 2008).

Rock bream (*Oplegnathus fasciatus*) is one of the most important fish species in Korean seafood industry and mainly utilized for popular Japanese sashimi. Due to the high demand, rock breams are being cultured in mariculture systems in South Korea. However, the production declines drastically due to the infections by bacteria and viruses in culture systems.

Fig. 9. The Rock Bream (*Oplegnathus fasciatus*)

In recent years, mass mortalities occurred in rock bream farms due to bacterial pathogens *Edwardsiella tarda* and *Streptococcus iniae* (Park Busan (Korea R.)) n.d.) and by the rock bream iridovirus (RBIV) (Jung & Oh 2000). *E. tarda* is a Gram-negative rod, facultative anaerobic bacteria, possessing a flagella for motility. The infection of *E. tarda* causes Edwardsiellosis. *S. iniae* is a Gram-positive, sphere-shaped bacterium identified as one of the severe fish pathogen, causes Streptococcicosis. The RBIV is a cytoplasmic, icosahedral, enveloped double stranded DNA virus, targeting several organs including gill, liver, kidney, spleen, heart, stomach, intestine, muscle, eye and brain (Kyung Choi et al. 2006; Shinmoto et al. 2009; Zhang et al. 2013).

Free During a pathogenic infection, it's no surprise that ROS are generated and should be mediated by the stock of enzymes present in the cellular matrix or organelles. Glutaredoxins tend to play a major part of antioxidant process and expectations are high if the pathway was understood properly in an important fish species, the Rock Bream. Previous studies have been conducted on several organisms such as yeast, human, fungi and Chinese honeybee but the knowledge on how GLRX1 acts on teleostean systems are yet to be carried out. With this phenomena at stake, developing a disease management strategy for commercially important fish species will definitely be accountable against taking step towards minimizing production loss.

2. MATERIALS AND METHODS

2.1 Experimental animal rearing

The animals (Rock bream fish) used for the experiment were provided by the National Fisheries Research and Development Institute, Republic of Korea. The selected animals had an average weight of 50 g and were acclimatized for a period of one week before the experiments. Factors such as temperature (22–24°C) and salinity (34 ± 0.6 psu) were maintained constantly and the rock breams were fed with commercially available feed during the acclimatization period.

2.2 Tissue Collection and cDNA synthesis

After the acclimatization period, whole blood (~1 mL/fish) was collected from caudal fin of fish using separate sterilized syringes and the samples were immediately centrifuged at 3000× g for 10 min at 4 °C to separate the blood cells from the plasma. The cells were subsequently snap-frozen in liquid nitrogen. Also the brain, gill, head kidney, heart, intestine, kidney, liver, muscle, skin, and spleen were excised from the sampled fish and immediately snap-frozen in liquid nitrogen furthermore stored at -80 °C for total RNA extraction.

Total RNA was extracted from pooled brain, gill, head kidney, heart, intestine, kidney, liver, muscle, skin, and spleen tissues using TRIzol reagent (Sigma–Aldrich), according to the manufacturer's protocol. Purified RNA samples were diluted to 1 μg/μL, and 2.5 μg of RNA from each tissue was used for cDNA synthesis using the PrimeScript™ First Strand cDNA Synthesis Kit (TaKaRa Bio Inc., Japan) following the manufacturer's protocol. The resulting cDNA was diluted 40-fold (total 800 μL) prior to storage at −20 °C.

제주대학교 중앙도서관
JEJU NATIONAL UNIVERSITY LIBRARY

2.3 Pathogenic Challenge

In order to study the time course expression patterns of RbGLRX1 under pathogenic stress, immune stimulation experiments were conducted with several stimulants and possible pathogens of rock bream from both bacteria and viruses. Independent groups of rock breams were administered a single intraperitoneal (i.p.) injection of 100 μL each of RBIV in PBS (10^3 TCID$_{50}$), or live *E. tarda* in PBS (5×10^6 CFU/mL) or *S. iniae* in (1×10^5 CFU/μL).

For all the above challenges, three fish were used at each time point and PBS-injected animals were used as controls. Tissues (blood, spleen, liver, and head kidney) from the control PBS-injected and immune-challenged animals were collected at post-injection (p.i.) time points of 3, 6, 12, 24 and 48 h. Total RNA was extracted from the corresponding tissues and cDNA synthesis was performed as in the previous section.

2.4 Tissue-specific gene expression analysis by qPCR

To detect the normal tissue distribution of RbGLRX1 expression, qRT-PCR was conducted for 11 selected tissues (blood, brain, gill, head kidney, heart, intestine, kidney, liver, muscle, skin, and spleen). Gene-specific primers for RbGLRX1 was designed according to MIQE guidelines, with 50% GC content, 60 °C Tm. The 10 μL reaction volume consisted of 3 μL of diluted cDNA from the particular tissue, 7 μL of 2× TaKaRa ExTaq SYBR Green premix containing 0.4 μL of each primer (RbGLRX1-L and RbGLRX1-R), and 1.6 μL of double-deionized (dd) H$_2$O. qRT-PCR was performed using the Dice™ Real time system thermal cycler (TP800; TaKaRa, Japan) with PCR conditions of 95 °C for 10 s; 35 cycles of 95 °C for 5 s, 58 °C for 10 s, and 72 °C for 20 s; and a final cycle of 95 °C for 15 s, 60 °C for 30 s, and 95 °C for 15 s. Each assay was triplicated.

2.5 Relative quantification of RbGLRX1 mRNA expression

The quantification of RbGLRX1 transcript patterns in pathogenic challenge was performed via qTR-PCR using the Real Time System TP800 Thermal Cycler Dice™ (TaKaRa, Japan) with the fluorescent agent SYBR Green as mentioned in Section 2.4 and using cDNA synthesized from the pathogenic challenge.

2.6 Identification of the cDNA sequence

Using a previously described rock bream cDNA sequence database (Lee et al. 2011) and with the use of Basic Local Alignment Search Tool (BLAST) (http://blast.ncbi.nlm.nih.gov/Blast.cgi) the full-length cDNA sequence homologous to Glutaredoxin 1 was identified in Rock bream and designated as *RbGLX1*.

2.7 Characterization of RbGLRX1

2.7.1 *In-silico* characterization of RbGLRX1

The amino acid sequence was deduced from the cDNA by DNAssist 2.2 program and it was also used to determine physiochemical properties of RbGLRX1. With the use of the SignalP 4.1 online server the signal peptide and the respective cleavage site was predicted. Distinctive domains of RbGLRX1 were predicted with the use of SMART online server (http://smart.embl-heidelberg.de) and NCBI-CDD server (http://www.ncbi.nlm.nih.gov/Structure/cdd/wrpsb.cgi). Orthologous sequences of RbGLRX1 were retrieved by the BLAST search tool and subsequently analyzed by ClustalW2 (http://www.Ebi.ac.uk/Tools/clustalw2) program and EMBOSS needle (http://www.Ebi.ac.uk/Tools/emboss/align) to obtain the multiple sequence alignment and pairwise sequence alignment respectively. The phylogenetic relationship was mapped using the Neighbor-joining method in Molecular Evolutionary Genetics Analysis (MEGA) software version

32

6 and 5000 bootstrap trials were performed to determine the confidence value with respect to RbGLRX1 family members in various taxonomic classes.

2.7.2 Expression and purification of the putative Recombinant RbGLRX1 protein

Two sequence-specific forward and reverse primers (Table 3) were designed with EcoRI and HindIII restriction sites, respectively, and ligated to the 5′ ends to amplify the cDNA region corresponding to the mature RbGLRX1 peptide. The PCR reaction was conducted in a 50 µL reaction mixture by adding 5 µL of 10× Ex Taq Buffer, 4 µL of 2.5 mM dNTPs, 40 pmol of each primer, 50 ng of blood cDNA and 5 U of Ex *Taq* polymerase (TaKaRa). The PCR profile was as follows: an initial denaturation of 94°C for 3 min; 35 cycles of amplification at 94°C for 30 s, 59°C for 30 s, and 72°C for 1.5 min; and a final extension at 72°C for 5 min. Subsequently, the resulting PCR products were run on an 1% agarose gel, and purified using the Accuprep™ gel purification kit (Bioneer-Korea) according to the manufacturer's instructions.

Table 3 Description of primers used in the study of RbGLRX1

Name	Application	Sequence (5′ →3′)
RbGLRX1-L	qPCR of *GLRX1*	GCCCACCTACCCTCAGCTATATGT
RbGLRX1-R	qPCR of *GLRX1*	CCACATCTTGCAGCCTCCTTGTT
Rb-β-actin - L	qPCR	TCATCACCATCGGCAATGAGAGGT
Rb-β-actin - R	qPCR	TGATGCTGTTGTAGGTGGTCTCGT
RbGLRX1-SL	Cloning	GAGAGAgaattcATGGCGCAGTTCGTGCAGACTAAAATTA
RbGLRX1-SR	Cloning	GAGAGAaagcttTCACTGCAGGGCTCCAATACACT

The recombinant prokaryotic RbGLRX1 expression system was designed by using the pMAL™-C2X prokaryotic expression vector (New England Biolabs, Ipswich, MA, USA). Both the pMAL™-C2X vector and gel purified PCR product were simultaneously digested with EcoRI and HindIII endonucleases. Then, digested PCR fragments were inserted into the vector by ligating with the Mighty Mix DNA Ligation Kit (TaKaRa). The accuracy of the recombinant construct (pMAL-C2X/ RbGLRX1) was confirmed by sequencing the vector inserts at Macrogen-Korea. A, single clone, confirmed by sequencing, was selected and transformed into *Escherichia coli* BL21 (DE3) competent cells (Novagen).

The pMAL-C2X/ RbGLRX1 -transformed BL21 (DE3) cells were cultured in LB rich medium supplemented with 100 μg/mL ampicillin and 100 mM glucose and were incubated at 37°C until OD_{600} reached ∼0.3. Temperature was then adjusted to 20°C in to perform the protein induction. Once the OD_{600} reached ∼0.5, protein induction was performed by adding isopropyl-β-thiogalactopyranoside (IPTG) to the culture medium at a final concentration of 0.5 mM while maintaining the temperature at 20°C. The culture was further incubated for 12 h at 20°C. Cells were harvested by centrifugation at 3500 rpm for 30 min at 4°C. The cell pellet was resuspended in column buffer (20 mM Tris–HCl, pH 7.4, 200 mM NaCl) and stored overnight at -20°C. The following day, the cell suspension was thawed and sonicated on ice in the presence of lysozyme (1 mg/mL). The resultant cell lysate was centrifuged at $9000 \times g$ for 30 min at 4°C. The supernatant was carefully pipetted and loaded into a column packed with amylose resin, and allowed to pass through the resin using gravity flow (maltose affinity chromatography). The resin bound with protein was washed with a $10 \times$ volume of column buffer. Finally, proteins were eluted by adding elution buffer (column buffer + 10 mM maltose). The protein purification method was monitored in stepwise manner by collecting the sample fractions at different steps of the purification

procedure and running them on a 12% SDS–PAGE gel along with standard molecular-weight size marker (PageRuler Plus, Thermo Scientific) and stained with 0.05% Coomassie blue R-250. The protein concentration was measured by the Bradford protein assay (Bradford 1976). To overexpress the maltose binding protein (MBP), the aforementioned protocol was repeated with pMAL-C2X vector instead of pMAL-C2X/RbGLRX1 vector.

2.8 Measurement of Free Radical Scavenging Activity

2.8.1 DPPH radical scavenging activity

DPPH radical scavenging activity was measured using the method described by Nanjo et al. (Nanjo et al. 1996). Briefly, 60 μL of various concentrations of each enzymatic hydrolysate was added to 60 μL of DPPH (60 μM) in methanol solution. After mixing vigorously for 10 s, the solution was transferred to a 100 μL Teflon capillary tube, and the scavenging activity of each enzymatic hydrolysate on the DPPH radical was measured using an ESR spectrometer. The spin adduct was measured on an ESR spectrometer exactly 2 min later. The DPPH radical scavenging activity was expressed as IC_{50} value, corresponding to a concentration for scavenging 50% of DPPH radicals. Experimental conditions were as follows: central field, 3475 G; modulation frequency, 100 kHz; modulation amplitude, 2 G; microwave power, 5 mW; gain, 6.3×10^5 and temperature, 298 K.

2.8.2 Peroxyl radical scavenging activity

Peroxyl radicals were generated by 2, 2-azobis (2-amidinopropane) hydrochloride (AAPH). The PBS (pH 7.4) reaction mixtures containing 0.1 ml of 10 mM AAPH, 0.1 ml of 10 mM (4-pyridyl-1- oxide)-N-tert-butylnitrone (4-POBN), and 0.1 ml of the indicated concentrations of the

35

tested samples were incubated at 37 °C in a water bath for 30 min and then transferred to a 100 μL Teflon capillary tube. The spin adduct was recorded on an ESR spectrometer. The peroxyl radical scavenging activity was expressed as IC_{50} value, which means concentration for scavenging 50% of peroxyl radicals. Measurement conditions were as follows: central field, 3475 G; modulation frequency, 100 kHz; modulation amplitude, 2 G; microwave power, 1 mW; gain, 6.3×10^5 and temperature, 298 K.

2.9 Functional Studies to confirm the activity of RbGLRX1

2.9.1 Insulin Disulfide Reduction Activity Assay

In defining the RbGLRX1 antioxidant activity, the insulin disulfide reduction assay was performed with few alterations as previously described by Holmgren et al (Holmgren 1979) . The reactions were performed in a 96 well plate with four different experimental setups. Briefly, a 300 mL reaction mixture containing 1.0 mM EDTA, 0.13 mM insulin from bovine pancreas (Sigma-Aldrich), 0.1 M Tris-HCl (pH 7.0), 1 mM Glutathione (GSH; IMCO Corporation, Sweden) and RbGLRX1 recombinant protein at different concentrations was prepared. Reaction mixture excluding GSH was used as the negative control group and purified MBP was used as the control system. The reactions were initiated by adding the GSH into the reaction mixtures and precipitation of reduced insulin was monitored for 60 min at 25°C subsequently measuring the absorbance at 650 nm. The specific activity was calculated $\Delta OD650 \times min^{-1} \times 1000/\mu g$ of rRbGLRX1(Holmgren 1979). All experimental trials were carried out as triplicates and the average values were considered for the final calculations.

2.9.2 HED Assay

A fresh mixture of 0.7 mM β-hydroxyethyl disulfide (HED), 0.2 mM EDTA, 0.1 mg/mL BSA, 250 µM NADPH, 1 unit glutathione reductase, 1 mM GSH in 100 µL 50mM Hepes, 100 mM NaCl, pH=7.5 was incubated for 5 min. A 2 µL volume of purified apo glutaredoxin was then added to the assay mixture and the change of absorbance was monitored at 340 nm in 1 min intervals upto a time of 15 minutes. The average values were considered after measuring each time point 3 times.

3. RESULTS AND DISCUSSION

3.1 Sequence identification and bioinformatics analysis of RbGLRX1

The identified *RbGLRX1* was 833 bp in size, with a 24 bp 5′-untranslated region (UTR) and a 491 bp 3′-UTR. The ORF (318 bp) encodes a polypeptide of 105 amino acids with molecular mass of 11.5 kDa and the theoretical isoelectric point of 7.65. According to the results obtained from the NCBI-CDD and ExPASy-prosite analyses, the RbGLRX1 amino acid sequence possessed a typical glutaredoxin-1 domain including the GSH binding sites Lys^{19}, Cys^{22}, Tyr^{24}, Arg^{67}-Pro^{70} and Gly^{81} – Asp^{84}. A signal peptide sequence was absent from RbGLRX1 leading to the fact that GLRX1 is a cytosolic enzyme unlike its isoforms. However, mammalian GLRX2 contains a translocating signal which in turn has the capability to have both nuclear and mitochondrial isoforms (Lundberg et al. 2001).

3.2 Homology and phylogenetic analysis

According to our pairwise sequence alignment study, RbGLRX1 shared significant sequence compatibility with its teleostean GLRX1 counterparts with a similarity of 90.6 % and an identity of 93.4 % with large yellow croaker GLRX1 validating its homology to GLRX1 counterparts (Table 4). When RbGLRX1 was compared with characterized other vertebrate and invertebrate homologues (Fig. 10.), clear evident was seen in the classical conserved region of CPYC where two cysteines were separated by Proline and Tyrosine residues. The two thiol groups in this motif are the source of reducing equivalents for substrate reduction. These residues form reversible disulfide bond during catalysis and were shown to be the enzyme active site.

Table 4 Pairwise sequence comparison of RbGLRX1 homologues

Name of the species	Common Name	NCBI accession Number	Amino acids	Identity (%)	Similarity (%)
Larimichthys crocea	Large yellow croaker	ACC86114	106	90.6	93.4
Lates calcarifer	Barramundi perch	AFP50145	106	88.7	94.3
Dicentrarchus labrax	European seabass	CBN81974	105	86.8	93.4
Osmerus mordax	Rainbow smelt	ACI66582	106	84.9	95.3
Danio rerio	Zebrafish	ADM61584	105	73.3	83.8
Esox lucius	Northern pike	NP001096599	106	72.6	84
Ictalurus punctatus	Channel catfish	NP001185577	106	70.8	85.8
Salmo salar	Atlantic salmon	NP000091	106	69.8	84
Xenopus tropicalis	Tropical clawed frog	NP036970	107	57.9	70.1
Sus scrofa	Pig	NP031819	106	55.7	74.5
Homo sapiens	Human	NP005204	106	53.8	72.6
Python bivittatus	Burmese python	NP001028411	105	53.8	71.7
Mus musculus	House mouse	NP001099346	107	51.4	73.8
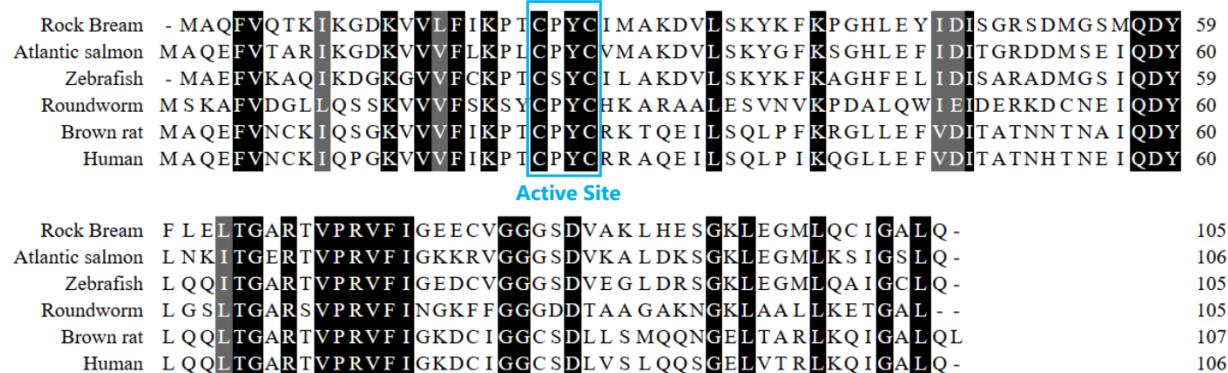
Fig. 10. Alignment of homologous GLRX1 amino acid sequences. Identical amino acid residues are darkly shaded, and similar amino acids are lightly shaded. The dashes represent gaps introduced to maximize alignment. The active site motif containing CPYC was encircled with blue lines. The GenBank accession numbers as follows: Atlantic salmon (ACI67872.1), Zebrafish (NP001005942.1), Roundworm (NP_490812.1), Brown rat (NP_071614.1), Human (BAA04769.1)

In order to further represent the evolutionary relationship of RbGLRX1 to other GLRX1 homologs, a phylogenetic tree was constructed (Fig. 11).

According to the branching patterns of the phylogenetic tree, RbGLRX1 exhibited the closest evolutionary relationship with its teleostean counterparts. According to the tree topology of teleostean GLRX1 counterparts, exclusively Rock bream and large yellow croaker GLRX1s were clustered in a close and independent clade whereas in accordance with the order, barramundi perch, rainbow smelt, and European seabass counterparts were clustered with increasing phylogenetic distance with that clade. Overall, the fish GLRX1s were clustered closely while

Amphibian, Birds, and Mammalians were each clustered separately. Collectively, deciphered phylogenetic relationship of RbGLRX1 with different homologues clearly asserts its evolutionary position among teleostan GLRX1s and its vertebrate ancestral origin.
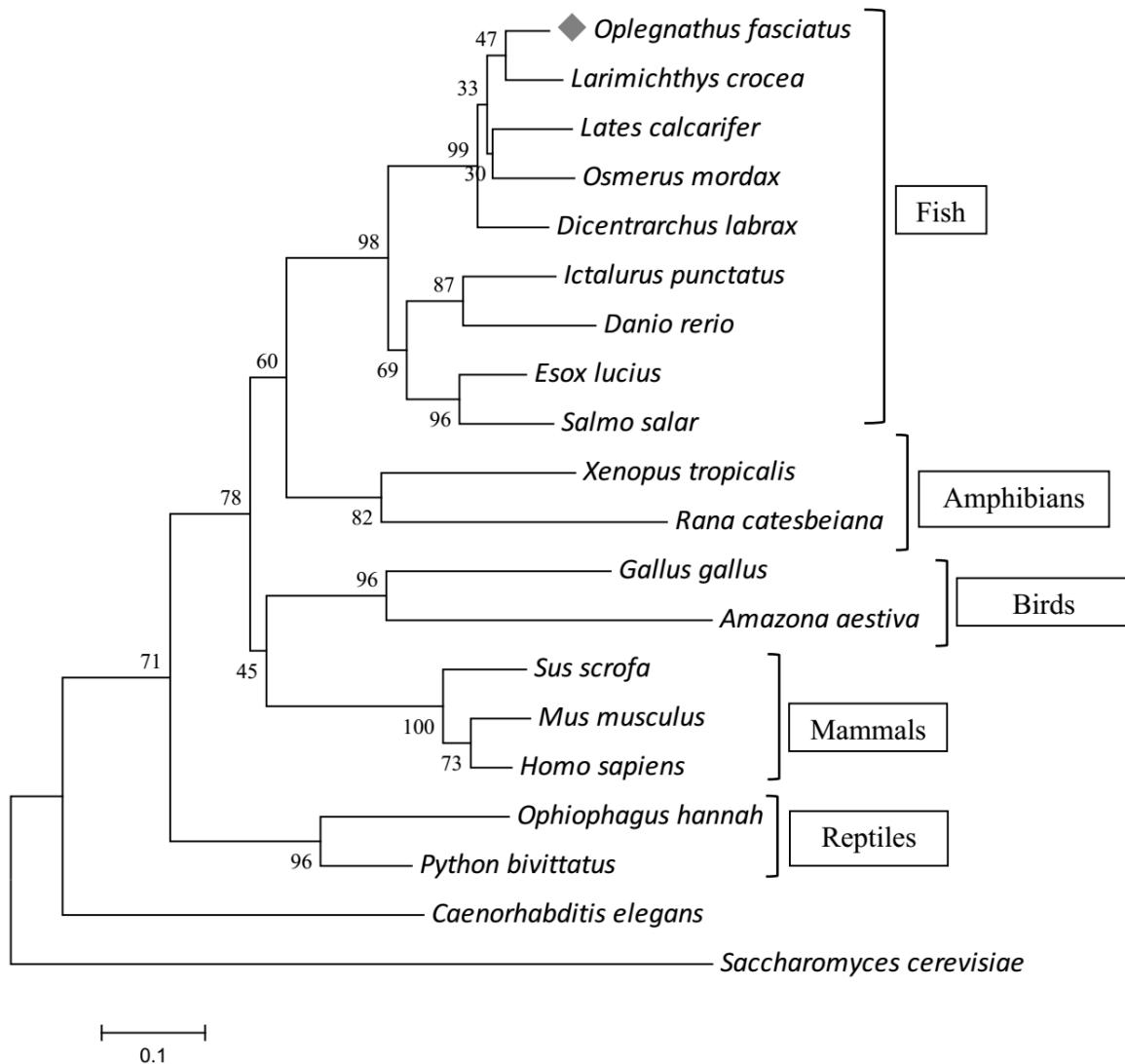

Fig. 11. Phylogenetic analysis of RbGLRX1 with selected, full-length GLRX1 amino acid sequences of several other species. The numbers at the nodes represent the bootstrap values for 5000 replicates. The Rock bream GLRX1homolog is denoted by a grey diamond symbol and the respective phylum were indicated with parenthesis. The NCBI-GenBank accession numbers of the amino acid sequences of the organisms used in the comparison are mentioned in Table 4 with

41

the exception of: *Rana catesbeiana* (ACO51672.1), *Ophiophagus Hannah* (ETE62116.1) *Gallus gallus* (NP_990491.1), *Amazona aestiva* (KQK81765.1) *Caenorhabditis elegans* (NP_490812.1), and *Saccharomyces cerevisiae* (P25373.1).

3.3 Tissue-specific gene expression analysis by qPCR

RbGLRX1 was ubiquitously expressed in 11 different tissues examined in healthy rock breams. A lower level of expression was detected in two tissues, muscle and skin where the muscle showed the lowest expression. However, kidney, gill, head kidney, heart, spleen, brain, intestine, displayed moderate expressions, whereas blood and liver tissues displayed high expression levels, blood showing the highest (∼15-fold compared with skin) mRNA expression (Fig. 12.). Overall, the obtained results reflect the diverse role of RbGLRX1 in a tissue-specific manner. After isolating GLRX from *Escherichia coli* several studies revealed its expression in liver, heart, thymus and placenta from several mammalian species including human, rat, calf and pig (Packer & Cadenas 1995; Wells et al. 1993). Strong expression levels of GLRX in the blood may be due to the high oxidative stress occurs in red blood cells while being as the main oxygen carriers in many organisms (MILLS 1957). Blood, spleen and kidney contains macrophages cells which are involved in the effector mechanisms such as phagocytosis to eliminate the invading pathogens which produces scores of ROS (Esteban et al. 2015; Secombes & Wang 2012; Segal 2005; Uribe et al. 2011). Liver, the metabolic center of ROS production also displayed high expression levels as expected. The expression pattern with respect to tissues clearly indicate the involvement if GLRX1 in immune related activities.
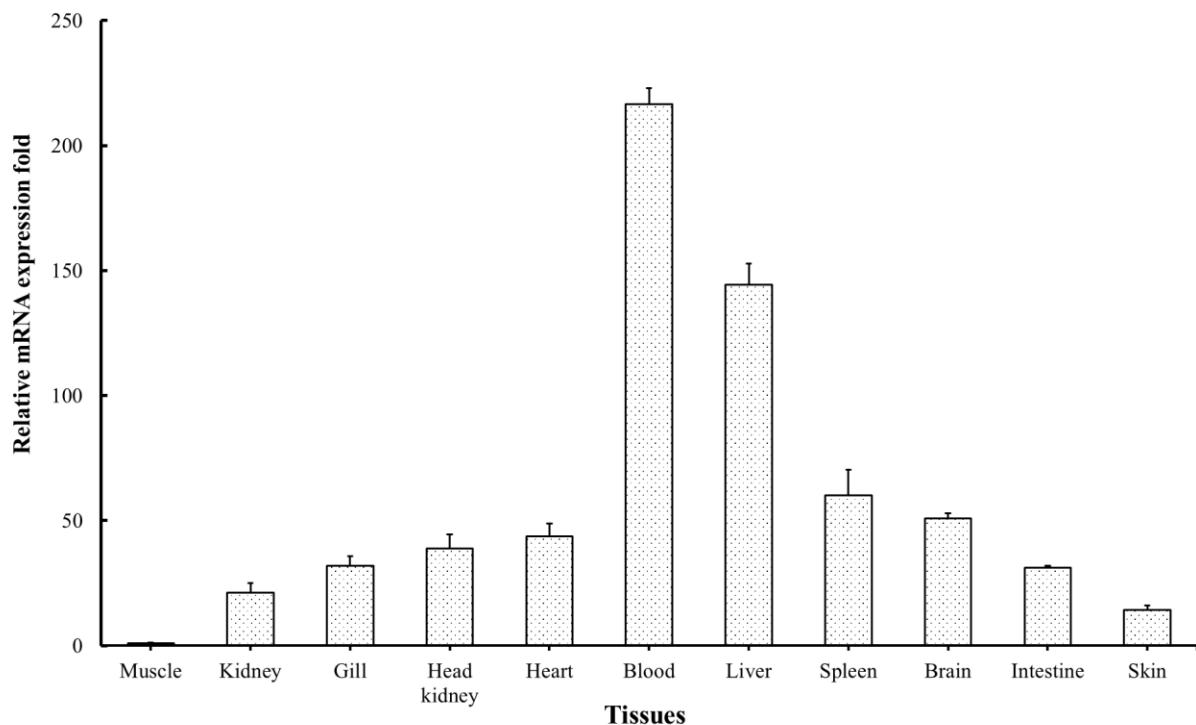
Fig. 12. Tissue-specific mRNA expression of the RbGLRX1 in healthy rock breams. Analysis of the mRNA level was carried out by qPCR and relative expressions were calculated compared to the mRNA level detected in muscle. Data are represented as means ± standard deviation (n = 3).

3.4 Transcriptional expression post-immune challenges

In order to evaluate the immunological potential in rock bream in response to pathogenic stress, expressional modulation of RbGLRX1 was analyzed in blood from rock bream after being treated with RBIV, *E. tarda* and *S. iniae* so as to emulate a viral or bacterial infection, respectively.

As detected by our qPCR assays, significant modulation of RbGLRX1 was noted in blood as well as liver tissues in response to the live bacterial and viral infection. Upon the viral infection, mRNA expression of RbGLRX1 was up-regulated in the blood tissues with ~ 1.5 fold compared

43

to its basal level (0 h post infection (p.i.)) at 3 h p.i. with a significant (P < 0.05) down-regulation at 12 h p.i (Fig. 13A). Bacterial infections of *E. tarda* and *S. iniae* displayed somewhat similar expression patterns. RbGLRX1 was expressed around 2 fold than the basal level at 6 h p.i. and a surge at 48 h p.i. after a sudden significant downregulation at 12 h p.i. on *E.tarda* immune challenge on rock bream blood. In the same tissue, *S. iniae* similarly trailed similar expression patterns with significant upregulations at 6, 12 and 48 h p.i. with 6 h p.i. being the highest.
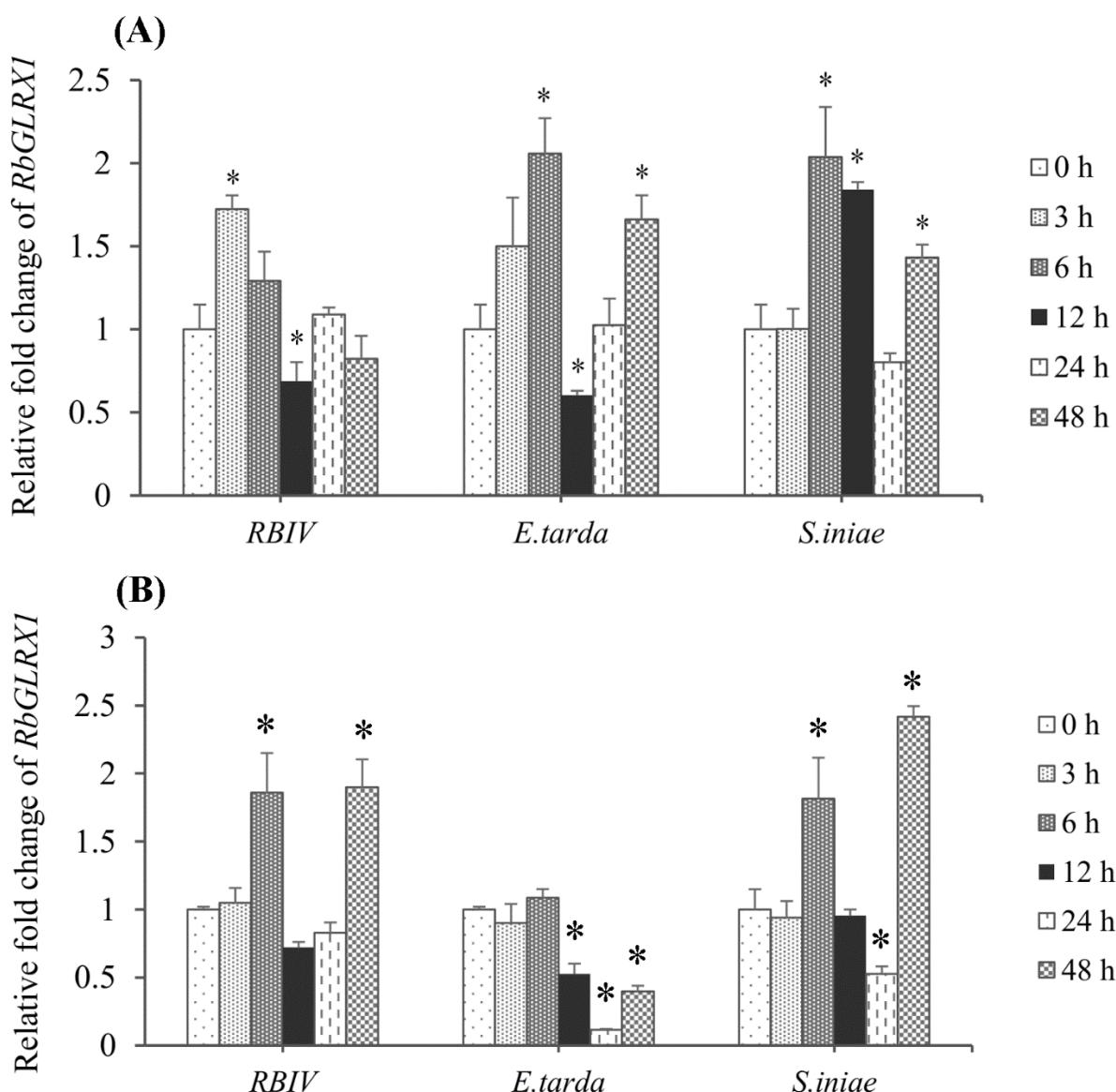
Fig. 13. RbGLRX1 expression analysis after RBIV, *E. tarda* and *S. iniae* challenge in (A) blood and (B) Liver tissues. Relative mRNA expression was calculated by the $2^{-\Delta\Delta Ct}$ method relative to PBS-injected controls and normalized with the same, with β-actin as the reference gene. Data shown with the asterisk indicates significant expression levels at $P < 0.05$.

Interestingly, liver showed noticeable transcriptional modulation exclusively with inductive transcriptional responses against the infection at middle and late phase p.i. (6 h and 48 h p.i.), in which more pronounced fold increase (~ 2 fold) was observed at 12 h p.i. compared to the basal level on RBIV and *S. iniae* infection (Fig. 13B). Conversely, infection of *E. tarda* only revealed downregulations especially during the middle and later stage (12 h and 48 h p.i.).

Overall, in comparison with the transcriptional responses of blood and liver, marked modulation of RbGLRX1 could be observed in blood than liver, compared to its basal level expression. The mid and late phase RbGLRX1 up-regulation may cause after the initial phagocytosis once the live bacterial infection takes place, subsequently regulating the redox potential via their antioxidant and free radical scavenging property.

3.5 Free Radical Scavenging Activity

DPPH is a stable radical widely used to assess the free radical scavenging activity of antioxidant systems (Sánchez-Moreno et al. 2006). The RbGLRX1 showed significant DPPH radical scavenging activity (IC$_{50}$, 1.91 ± 0.01 mg/mL) in a concentration dependent manner. The parameters IC$_{50}$, which reflects 50% depletion of the initial DPPH radical and the time needed to reach the steady state at IC$_{50}$ concentration. (Fig. 14A). Alternatively, peroxyl radicals generated by AAPH were measured after treatment with recombinant protein samples by an ESR

spectrometer. RbGLRX1 (IC_{50}, 0.38 ± 0.004 mg/mL) demonstrated to possess significant peroxyl radical scavenging activity too. (Fig. 14B).
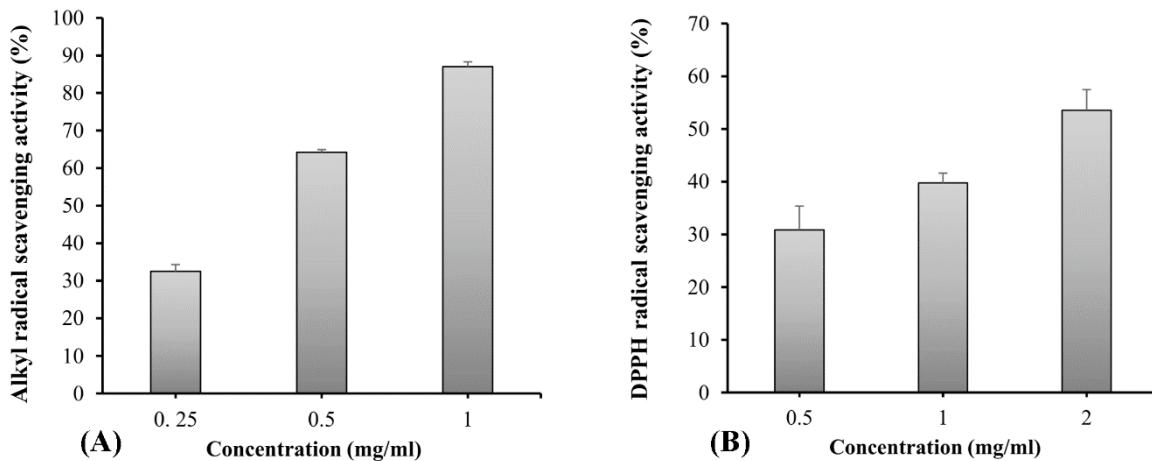

Fig. 14. (A) Alkyl and (B) DPPH radical scavenging activities of RbGLRX1 at different concentrations of recombinant proteins. Data are presented as mean of duplicate samples, and the error bars represented the standard deviations.

3.6 Functional Studies on RbGLRX1

3.6.1 Insulin Disulfide reduction assay

GLRX1 is a typical CPYC type GLRX which is reduced by GSH and can catalyze reduction of insulin, DHA and glutathionylated substrates (Gao et al. 2010). Insulin disulfide bonds are very efficiently reduced by Thioredoxins (TRXs) (Holmgren 1979). Although much less efficient, CPYC-type GRXs are known to catalyze insulin reduction using DTT or GSH as electron donor (Mannervik et al. 1983). rRbGLRX1 indicated significant activity in the insulin reduction assay with the two different concentrations of the recombinant protein (Fig. 15.). The results were in par with previous studies on GLRX1 of *Chlamydomonas reinhardtii* (Gao et al. 2010).

46

Formation of a mixed disulfide between a protein thiol and glutathione, i.e. S-glutathionylation (or S-glutathiolation), is considered a potential regulatory mechanism especially under oxidative stress (Shelton et al. 2005; Ghezzi 2005; Klatt & Lamas 2000). Most enzymes with an active cysteine site lose activity upon S-glutathionylation and regain activity when reduced by thiols. While the cellular mechanism of S-glutathionylation remains unresolved, deglutathionylation is known to be catalyzed by glutaredoxins (Shelton et al. 2005). Glutaredoxins 1 and 2 are disulfide-dithiol oxidoreductases localized in cytosol and mitochondrial matrix, respectively (Fernandes & Holmgren 2004). They catalyze the transfer of a glutathione moiety from an S-glutathionylated protein to glutathione.
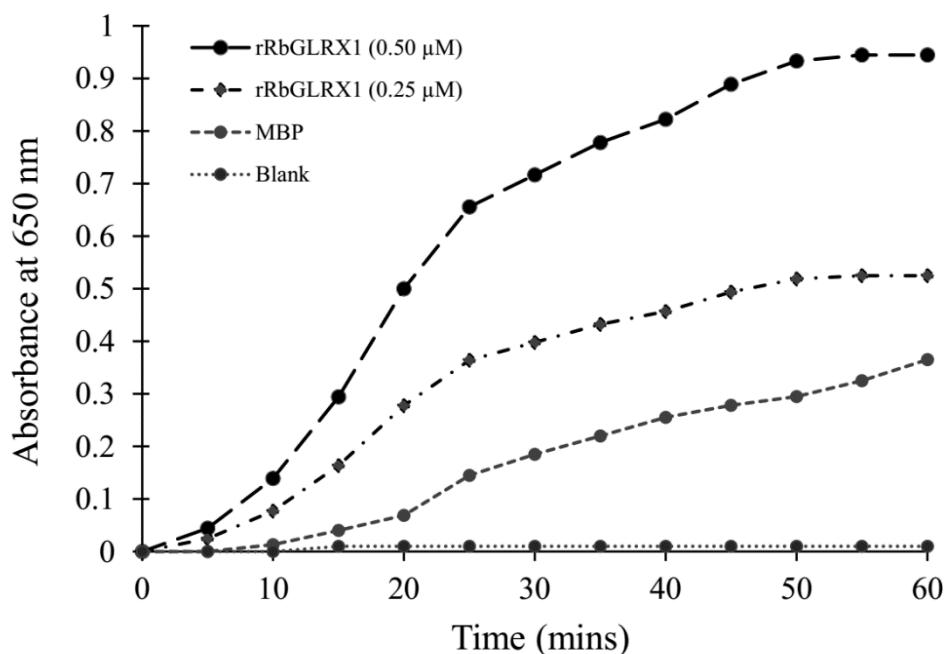
**Fig. 15.** Insulin disulfide reductase activity of RbGLRX1. The rate of insulin reduction was assessed by measuring the turbidity at 650 nm in reaction assays containing 1 mM GSH in the presence of 2.5 and 5 µM Rock bream GLRX1in presence or absence of GSH. The MBP was added instead of recombinant protein in the control group (MBP) and negative control group was

제주대학교 중앙도서관
JEJU NATIONAL UNIVERSITY LIBRARY

without GSH. The blank group lacked GSH and recombinant proteins but only column buffer. Data are presented as mean values (n = 3) for all experiments.

3.6.2 HED Assay

Deglutathionylation activities of GLRXs were measured with the standard HED assay. GLRX activity is followed as the oxidation of NADPH in a coupled system with GSH and glutathione reductase (GR). The substrate of GLRX, the glutathionylated β-mercaptoethanol (β-ME-SG), is formed during the initial pre-incubation (5 mins) where HED reacts with GSH. The reaction proceeds in two steps. Initially, GLRX performs a primary nucleophilic attack on the β-ME-SG mixed disulfide producing GLRX-SG and releasing the deglutathionylated substrate. In the later step, reaction of GSH with GLRX-SG allows reduction of GLRX and releases GSSG. This second step is the rate-limiting step of the reaction (Gao et al. 2010). The results from the graph (Fig. 16.) clearly displays the activity of rRbGLRX1 when GSH was added and the MBP does not show any indication of reducing the substrate thus maintaining the initial level of absorbance reduction. According to previous studies, GLRX is the most specific and efficient enzyme of the thioredoxin superfamily to catalyze the reversible thiolation and dethiolation of protein cysteinyl thiols with glutathione (Gravina & Mieyal 1993; Jung & Thomas 1996).

48
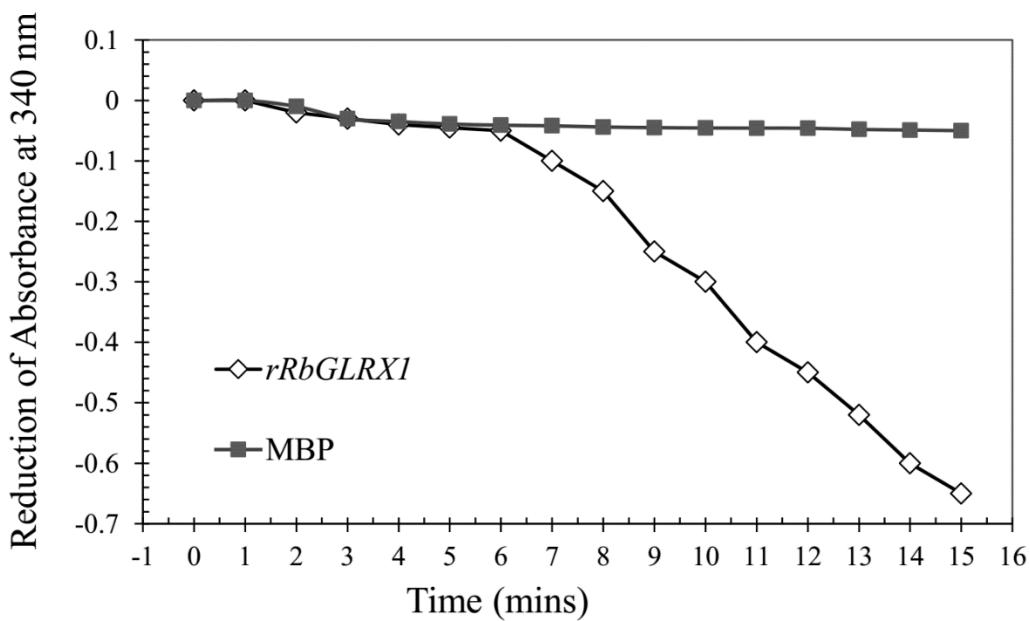
Fig. 16. HED assays where reduction of the disulfide bond in HED by rRbGLRX1. After 5 min of incubation, GSH was added, and the reaction was monitored at 340 nm. Solid blocks represent the reaction in the presence of MBP while the hollow box represents reaction with rRbGLRX1.

4. CONCLUSION

In conclusion, the full-length cDNA encoding GLRX1 was identified from *O. fasciatus* and RbGLRX1 mRNA were constitutively expressed in the tested tissues, and transcripts were up-regulated at 24 h after viral and bacterial challenges. Alkyl and Peroxyl scavenging activities were displayed by the rRBGLRX1 and positive results were obtained for specific Insulin Disulfide reduction assay and classical HED assay. These results suggested that RbGLRX1 perhaps played an essential role in maintenance of redox balance in the cytosol while defending the immune system of the host by pathogenic infections.

REFERENCES

Ahn, S.J. et al., 2013. Olive flounder (Paralichthys olivaceus) cystatin B: cloning, tissue distribution, expression and inhibitory profile of piscine cystatin B. *Comparative biochemistry and physiology. Part B, Biochemistry & molecular biology*, 165(3), pp.211–8. Available at: http://www.ncbi.nlm.nih.gov/pubmed/23648289.

Bai, J. et al., 2006. Molecular cloning, sequencing, expression of Chinese sturgeon cystatin in yeast Pichia pastoris and its proteinase inhibitory activity. *Journal of Biotechnology*, 125(2), pp.231–241. Available at: http://linkinghub.elsevier.com/retrieve/pii/S0168165606001647.

Birben, E. et al., 2012. Oxidative Stress and Antioxidant Defense. *World Allergy Organization Journal*, 5(1), pp.9–19. Available at: http://www.waojournal.org/content/5/1/9.

Bode, W. et al., 1988. The 2.0 A X-ray crystal structure of chicken egg white cystatin and its possible mode of interaction with cysteine proteinases. *The EMBO journal*, 7(8), pp.2593–9. Available at: http://www.ncbi.nlm.nih.gov/pubmed/3191914.

Bode, W. & Huber, R., 2000. Structural basis of the endoproteinase-protein inhibitor interaction. *Biochimica et biophysica acta*, 1477(1–2), pp.241–52. Available at: http://www.ncbi.nlm.nih.gov/pubmed/10708861.

Bradford, M.M., 1976. A rapid and sensitive method for the quantitation of microgram quantities of protein utilizing the principle of protein-dye binding. *Analytical biochemistry*, 72, pp.248–54. Available at: http://www.ncbi.nlm.nih.gov/pubmed/942051.

Brown, W.M. & Dziegielewska, K.M., 1997. Friends and relations of the cystatin superfamily--new members and their evolution. *Protein science : a publication of the Protein Society*, 6(1), pp.5–12. Available at: http://www.ncbi.nlm.nih.gov/pubmed/9007972.

Campanella, J.J., Bitincka, L. & Smalley, J., 2003. No Title. *BMC Bioinformatics*, 4(1), p.29. Available at: http://bmcbioinformatics.biomedcentral.com/articles/10.1186/1471-2105-4-29.

Chapman, H.A., Riese, R.J. & Shi, G.P., 1997. Emerging roles for cysteine proteases in human biology. *Annual review of physiology*, 59, pp.63–88. Available at: http://www.ncbi.nlm.nih.gov/pubmed/9074757.

Cornwall, G.A. & Hsia, N., 2003. A new subgroup of the family 2 cystatins. *Molecular and Cellular Endocrinology*, 200(1–2), pp.1–8.

D'Autréaux, B. & Toledano, M.B., 2007. ROS as signalling molecules: mechanisms that generate specificity in ROS homeostasis. *Nature reviews. Molecular cell biology*, 8(10), pp.813–24. Available at: http://www.ncbi.nlm.nih.gov/pubmed/17848967.

Elvitigala, D.A.S. et al., 2015. A teleostan homolog of catalase from black rockfish (Sebastes schlegelii): Insights into functional roles in host antioxidant defense and expressional responses to septic conditions. *Fish and Shellfish Immunology*, 44(1), pp.321–331.

Esteban, M. et al., 2015. Phagocytosis in Teleosts. Implications of the New Cells Involved. *Biology*, 4(4), pp.907–922. Available at: http://www.mdpi.com/2079-7737/4/4/907.

Fernandes, A.P. & Holmgren, A., 2004. Glutaredoxins: glutathione-dependent redox enzymes with functions far beyond a simple thioredoxin backup system. *Antioxidants & redox signaling*, 6(1), pp.63–74. Available at: http://www.ncbi.nlm.nih.gov/pubmed/14713336.

Gao, X.H. et al., 2010. Biochemical characterization of glutaredoxins from Chlamydomonas reinhardtii: Kinetics and specificity in deglutathionylation reactions. *FEBS Letters*, 584(11), pp.2242–2248. Available at: http://dx.doi.org/10.1016/j.febslet.2010.04.034.

Ghezzi, P., 2005. Regulation of protein function by glutathionylation. *Free radical research*, 39(6), pp.573–80. Available at: http://www.ncbi.nlm.nih.gov/pubmed/16036334.

Gravina, S.A. & Mieyal, J.J., 1993. Thioltransferase is a specific glutathionyl mixed disulfide oxidoreductase. *Biochemistry*, 32(13), pp.3368–76. Available at: http://www.ncbi.nlm.nih.gov/pubmed/8461300.

Gromer, S., Urig, S. & Becker, K., 2004. The thioredoxin system--from science to clinic. *Medicinal research reviews*, 24(1), pp.40–89. Available at: http://www.ncbi.nlm.nih.gov/pubmed/14595672.

Grzonka, Z. et al., 2001. Structural studies of cysteine proteases and their inhibitors. *Acta biochimica Polonica*, 48(1), pp.1–20. Available at: http://www.ncbi.nlm.nih.gov/pubmed/11440158.

Han, H.-J. et al., 2011. Atypical Aeromonas salmonicida infection in the black rockfish, Sebastes schlegeli Hilgendorf, in Korea. *Journal of fish diseases*, 34(1), pp.47–55. Available at: http://www.ncbi.nlm.nih.gov/pubmed/21166824.

Hartmann, S. et al., 2002. Cystatins of filarial nematodes up-regulate the nitric oxide production of interferon-gamma-activated murine macrophages. *Parasite immunology*, 24(5), pp.253–62. Available at: http://www.ncbi.nlm.nih.gov/pubmed/12060319.

Hensley, K. et al., 2000. Reactive oxygen species, cell signaling, and cell injury. *Free radical biology & medicine*, 28(10), pp.1456–62. Available at: http://www.ncbi.nlm.nih.gov/pubmed/10927169.

Holmgren, A., 1979. Thioredoxin catalyzes the reduction of insulin disulfides by dithiothreitol and dihydrolipoamide. *The Journal of biological chemistry*, 254(19), pp.9627–32. Available at: http://www.ncbi.nlm.nih.gov/pubmed/385588.

Jon, 2012. PAPAIN, A PLANT ENZYME OF BIOLOGICAL IMPORTANCE: A REVIEW. *American Journal of Biochemistry and Biotechnology*, 8(2), pp.99–104. Available at: http://thescipub.com/abstract/10.3844/ajbbsp.2012.99.104.

Josiah Ochieng & Gautam Chaudhuri, 2010. Cystatin Superfamily. *Journal of Health Care for the Poor and Underserved*, 21(1A), pp.51–70. Available at: http://muse.jhu.edu/content/crossref/journals/journal_of_health_care_for_the_poor_and_un derserved/v021/21.1A.ochieng.html.

Jung, C.H. & Thomas, J.A., 1996. S-glutathiolated hepatocyte proteins and insulin disulfides as substrates for reduction by glutaredoxin, thioredoxin, protein disulfide isomerase, and glutathione. *Archives of biochemistry and biophysics*, 335(1), pp.61–72. Available at: http://www.ncbi.nlm.nih.gov/pubmed/8914835.

52

Jung, S.J. & Oh, M.J., 2000. Iridovirus-like infection associated with high mortalities of striped beakperch, Oplegnathus fasciatus (Temminck et Schlegel), in southern coastal areas of the Korean peninsula. *Journal of Fish Diseases*, 23(3), pp.223–226. Available at: http://doi.wiley.com/10.1046/j.1365-2761.2000.00212.x.

Klatt, P. & Lamas, S., 2000. Regulation of protein function by S-glutathiolation in response to oxidative and nitrosative stress. *European journal of biochemistry*, 267(16), pp.4928–44. Available at: http://www.ncbi.nlm.nih.gov/pubmed/10931175.

Kyung Choi, S. et al., 2006. Organ distribution of red sea bream iridovirus (RSIV) DNA in asymptomatic yearling and fingerling rock bream (Oplegnathus fasciatus) and effects of water temperature on transition of RSIV into acute phase. *Aquaculture*, 256(1–4), pp.23–26. Available at: http://linkinghub.elsevier.com/retrieve/pii/S0044848606000664.

Lee, Y. et al., 2011. Molluscan death effector domain (DED)-containing caspase-8 gene from disk abalone (Haliotis discus discus): Molecular characterization and expression analysis. *Fish and Shellfish Immunology*, 30(2), pp.480–487. Available at: http://dx.doi.org/10.1016/j.fsi.2010.11.014.

Lillig, C.H. et al., 2005. Characterization of human glutaredoxin 2 as iron-sulfur protein: a possible role as redox sensor. *Proceedings of the National Academy of Sciences of the United States of America*, 102(23), pp.8168–73. Available at: http://www.ncbi.nlm.nih.gov/pubmed/15917333.

Lillig, C.H., Berndt, C. & Holmgren, A., 2008. Glutaredoxin systems. *Biochimica et Biophysica Acta - General Subjects*, 1780(11), pp.1304–1317.

Livak, K.J. & Schmittgen, T.D., 2001. Analysis of relative gene expression data using real-time quantitative PCR and the 2(-Delta Delta C(T)) Method. *Methods (San Diego, Calif.)*, 25(4), pp.402–8. Available at: http://www.ncbi.nlm.nih.gov/pubmed/11846609.

Lundberg, M. et al., 2001. Cloning and expression of a novel human glutaredoxin (Grx2) with mitochondrial and nuclear isoforms. *The Journal of biological chemistry*, 276(28), pp.26269–75. Available at: http://www.ncbi.nlm.nih.gov/pubmed/11297543.

Mannervik, B. et al., 1983. Relative contributions of thioltransferase-and thioredoxin-dependent systems in reduction of low-molecular-mass and protein disulphides. *Biochemical Journal*, 213(2), pp.519–523. Available at: http://www.ncbi.nlm.nih.gov/pmc/articles/PMC1152157/%5Cnhttp://www.ncbi.nlm.nih.gov/pmc/articles/PMC1152157/pdf/biochemj00347-0239.pdf.

Manuscript, A. & Superfamily, C., 2011. Cystatin Superfamily. , 21(615), pp.51–70.

Marletta, M.A., 1993. Nitric oxide synthase structure and mechanism. *The Journal of biological chemistry*, 268(17), pp.12231–4. Available at: http://www.ncbi.nlm.nih.gov/pubmed/7685338.

MILLS, G.C., 1957. Hemoglobin catabolism. I. Glutathione peroxidase, an erythrocyte enzyme which protects hemoglobin from oxidative breakdown. *The Journal of biological chemistry*, 229(1), pp.189–97. Available at: http://www.ncbi.nlm.nih.gov/pubmed/13491573.

Nanjo, F. et al., 1996. Scavenging effects of tea catechins and their derivatives on 1,1-diphenyl-

2-picrylhydrazyl radical. *Free radical biology & medicine*, 21(6), pp.895–902. Available at: http://www.ncbi.nlm.nih.gov/pubmed/8902534.

Nordberg, J. & Arnér, E.S., 2001. Reactive oxygen species, antioxidants, and the mammalian thioredoxin system. *Free radical biology & medicine*, 31(11), pp.1287–312. Available at: http://www.ncbi.nlm.nih.gov/pubmed/11728801.

P.A. Pemberton, 2006. No Title. *Encyclopedia of Respiratory Medicine*, pp.511–517.

Packer, L. & Cadenas, E., 1995. *Biothiols in health and disease*, Available at: Mike Law 3-3-98 x7837.

Park Busan (Korea R.)), S.I. (Pukyon. N.U., Disease control in Korean aquaculture. *Fish Pathology (Japan)*, v. 44.

Premachandra, H.K.A., Whang, I., et al., 2012. Cystatin B homolog from rock bream Oplegnathus fasciatus: genomic characterization, transcriptional profiling and protease-inhibitory activity of recombinant protein. *Comparative biochemistry and physiology. Part B, Biochemistry & molecular biology*, 163(1), pp.138–46. Available at: http://www.ncbi.nlm.nih.gov/pubmed/22626887.

Premachandra, H.K.A. et al., 2013. Expression profile of cystatin B ortholog from Manila clam (Ruditapes philippinarum) in host pathology with respect to its structural and functional properties. *Fish & shellfish immunology*, 34(6), pp.1505–13. Available at: http://www.ncbi.nlm.nih.gov/pubmed/23528873.

Premachandra, H.K.A., Wan, Q., et al., 2012. Genomic characterization and expression profiles upon bacterial infection of a novel cystatin B homologue from disk abalone (Haliotis discus discus). *Developmental and comparative immunology*, 38(4), pp.495–504. Available at: http://www.ncbi.nlm.nih.gov/pubmed/22878425.

Rawlings, N.D. & Barrett, A.J., 1999. MEROPS: The peptidase database. *Nucleic Acids Research*, 27(1), pp.325–331.

Rodríguez-Manzaneque, M.T. et al., 1999. Grx5 glutaredoxin plays a central role in protection against protein oxidative damage in Saccharomyces cerevisiae. *Molecular and cellular biology*, 19(12), pp.8180–90. Available at: http://www.ncbi.nlm.nih.gov/pubmed/10567543.

Rouhier, N., Lemaire, S.D. & Jacquot, J.-P., 2008. The role of glutathione in photosynthetic organisms: emerging functions for glutaredoxins and glutathionylation. *Annual review of plant biology*, 59, pp.143–66. Available at: http://www.ncbi.nlm.nih.gov/pubmed/18444899.

Rudenskaya, G.N. & Pupov, D. V., 2008. Cysteine proteinases of microorganisms and viruses. *Biochemistry (Moscow)*, 73(1), pp.1–13. Available at: http://link.springer.com/10.1134/S000629790801001X.

Rudneva, I.I., 1999. Antioxidant system of Black Sea animals in early development. *Comparative biochemistry and physiology. Part C, Pharmacology, toxicology & endocrinology*, 122(2), pp.265–71. Available at: http://www.ncbi.nlm.nih.gov/pubmed/10190054.

Sánchez-Moreno, C. et al., 2006. Nutritional characterisation of commercial traditional pasteurised tomato juices: carotenoids, vitamin C and radical-scavenging capacity. *Food Chemistry*, 98(4), pp.749–756. Available at: http://linkinghub.elsevier.com/retrieve/pii/S0308814605005789.

Secombes, C.J. & Wang, T., 2012. The innate and adaptive immune system of fish. In *Infectious Disease in Aquaculture*. Elsevier, pp. 3–68. Available at: http://linkinghub.elsevier.com/retrieve/pii/B9780857090164500015.

Segal, A.W., 2005. HOW NEUTROPHILS KILL MICROBES. *Annual Review of Immunology*, 23(1), pp.197–223. Available at: http://www.annualreviews.org/doi/10.1146/annurev.immunol.23.021704.115653.

Seifried, H.E. et al., 2007. A review of the interaction among dietary antioxidants and reactive oxygen species. *The Journal of nutritional biochemistry*, 18(9), pp.567–79. Available at: http://www.ncbi.nlm.nih.gov/pubmed/17360173.

Shelton, M.D., Chock, P.B. & Mieyal, J.J., 2005. Glutaredoxin: role in reversible protein s-glutathionylation and regulation of redox signal transduction and protein translocation. *Antioxidants & Redox Signaling*, 7(3–4), pp.348–366. Available at: http://www.ncbi.nlm.nih.gov/pubmed/15706083.

Shinmoto, H. et al., 2009. Phenotypic diversity of infectious red sea bream iridovirus isolates from cultured fish in Japan. *Applied and Environmental Microbiology*, 75(11), pp.3535–3541.

Stubbs, M.T. et al., 1990. The refined 2.4 A X-ray crystal structure of recombinant human stefin B in complex with the cysteine proteinase papain: a novel type of proteinase inhibitor interaction. *The EMBO journal*, 9(6), pp.1939–47. Available at: http://www.ncbi.nlm.nih.gov/pubmed/2347312.

Tamura, K. et al., 2013. MEGA6: Molecular Evolutionary Genetics Analysis version 6.0. *Molecular biology and evolution*, 30(12), pp.2725–9. Available at: http://www.ncbi.nlm.nih.gov/pubmed/24132122.

Thompson, J.D., Higgins, D.G. & Gibson, T.J., 1994. CLUSTAL W: improving the sensitivity of progressive multiple sequence alignment through sequence weighting, position-specific gap penalties and weight matrix choice. *Nucleic acids research*, 22(22), pp.4673–80. Available at: http://www.ncbi.nlm.nih.gov/pubmed/7984417.

Turk, D., 2001. Structure of human dipeptidyl peptidase I (cathepsin C): exclusion domain added to an endopeptidase framework creates the machine for activation of granular serine proteases. *The EMBO Journal*, 20(23), pp.6570–6582. Available at: http://emboj.embopress.org/cgi/doi/10.1093/emboj/20.23.6570.

Turk, Ï., Turk, V. & Turk, B., 2001. NEW EMBO MEMBER â€™ S REVIEW Lysosomal cysteine proteases : facts and opportunities. , 20(17).

Turk, V. et al., 2002. Lysosomal cathepsins: Structure, role in antigen processing and presentation, and cancer. *Advances in Enzyme Regulation*, 42, pp.285–303.

Turk, V. & Bode, W., 1991. The cystatins: protein inhibitors of cysteine proteinases. *FEBS*

letters, 285(2), pp.213–9. Available at: http://www.ncbi.nlm.nih.gov/pubmed/1855589.

Uribe, C. et al., 2011. Innate and adaptive immunity in teleost fish: a review. *Veterinární Medicína*, 56(10), pp.486–503. Available at: http://vri.cz/docs/vetmed/56-10-486.pdf.

Valko, M. et al., 2006. Free radicals, metals and antioxidants in oxidative stress-induced cancer. *Chemico-Biological Interactions*, 160(1), pp.1–40. Available at: http://linkinghub.elsevier.com/retrieve/pii/S0009279705004333.

Verdot, L. et al., 1999. Chicken cystatin stimulates nitric oxide release from interferon-gamma-activated mouse peritoneal macrophages via cytokine synthesis. *European journal of biochemistry*, 266(3), pp.1111–7. Available at: http://www.ncbi.nlm.nih.gov/pubmed/10583408.

Verdot, L. et al., 1996. Cystatins up-regulate nitric oxide release from interferon-gamma-activated mouse peritoneal macrophages. *The Journal of biological chemistry*, 271(45), pp.28077–81. Available at: http://www.ncbi.nlm.nih.gov/pubmed/8910420.

Vlamis-Gardikas, A. et al., 1997. Cloning, overexpression, and characterization of glutaredoxin 2, an atypical glutaredoxin from Escherichia coli. *Journal of Biological Chemistry*, 272(17), pp.11236–11243.

Vlamis-Gardikas, A. & Holmgren, A., 2002. Thioredoxin and glutaredoxin isoforms. *Methods in enzymology*, 347, pp.286–96. Available at: http://www.ncbi.nlm.nih.gov/pubmed/11898418.

Wells, W.W. et al., 1993. Thioltransferases. *Advances in enzymology and related areas of molecular biology*, 66, pp.149–201. Available at: http://www.ncbi.nlm.nih.gov/pubmed/8430514.

Xiao, P., Hu, Y. & Sun, L., 2010. Scophthalmus maximus cystatin B enhances head kidney macrophage-mediated bacterial killing. *Developmental and comparative immunology*, 34(12), pp.1237–41. Available at: http://www.ncbi.nlm.nih.gov/pubmed/20692286.

Yoon, Jong-Man ; Choi, Youn ; Kim, J.-Y., 2007. Genetic Differences and Variation in Black Rockfish (Sebastes schlegeli) and Hwanghae Rockfish (S. koreanus) from the Yellow Sea. *The Korean journal of genetics*, 29(4), pp.437–445.

Zapata, A. et al., 2006. Ontogeny of the immune system of fish. *Fish & shellfish immunology*, 20(2), pp.126–36. Available at: http://www.ncbi.nlm.nih.gov/pubmed/15939627.

Zavasnik-Bergant, T., 2008. Cystatin protease inhibitors and immune functions. *Frontiers in Bioscience*, Volume(13), p.4625. Available at: http://www.bioscience.org/2008/v13/af/3028/list.htm.

Zhang, B.-C. et al., 2013. Complete genome sequence and transcription profiles of the rock bream iridovirus RBIV-C1. *Diseases of aquatic organisms*, 104(3), pp.203–14. Available at: http://www.ncbi.nlm.nih.gov/pubmed/23759558.